

# The Impact of Climate Change on Hydro-meteorological Droughts Using Copula Functions

Zahra Fahimirad

University of Qom

Nazanin Shahkarami (✉ [n-shahkarami@araku.ac.ir](mailto:n-shahkarami@araku.ac.ir))

Arak University <https://orcid.org/0000-0002-4441-2571>

---

## Research Article

**Keywords:** Drought, climate change, aggregated index, PCA, Copula function

**Posted Date:** April 9th, 2021

**DOI:** <https://doi.org/10.21203/rs.3.rs-237122/v1>

**License:**   This work is licensed under a Creative Commons Attribution 4.0 International License.

[Read Full License](#)

---

# The Impact of Climate Change on Hydro-meteorological Droughts Using Copula Functions

Zahra Fahimirad\*, Nazanin Shahkarami\*\*†

## Abstract

Climate change has made many alterations to the Earth's climate, including hydro-climatic extreme events. For investigating the effect of climate change on hydro-meteorological droughts in the Kamal-Saleh dam basin in Markazi province, Iran, a new and comprehensive index was developed for accurate estimation of drought in a more realistic condition, for future climate conditions. This aggregate drought index (ADI) represents the main characteristics of meteorological and hydrological drought. Temperature and precipitation projections for future climates were simulated by five CMIP5 models and downscaled over the study area for the periods of 2050s (2040-2069) and 2080s (2070-2099) relative to the baseline period (1976-2005). By fitting five univariate distribution functions on drought severity and duration, proper marginal distributions were selected. The joint distribution of drought severity and duration was chosen from five types of copula functions. The results revealed that severe droughts are expected to occur frequently in a shorter period in the future.

**Keywords:** Drought, climate change, aggregated index, PCA, Copula function.

---

\* Graduate Student, Dept. of Civil Engineering, University of Qom, Qom, 3716146611, Iran. E-mail: [z.fahimirad70@gmail.com](mailto:z.fahimirad70@gmail.com)

† Corresponding author. Assistant Professor, Dept. of Civil Engineering, Arak University, Arak 38137, Iran. (<https://orcid.org/0000-0002-4441-2571>). E-mail: [n-shahkarami@araku.ac.ir](mailto:n-shahkarami@araku.ac.ir). (<https://orcid.org/0000-0002-4441-2571>)

## 1 Introduction

The unprecedented environmental and socio-economic impacts of climate change, have become undeniable in today's society. Recent researches have suggested that changes in the frequency of extreme events may be accompanied by climate change. In general, an increase in droughts, especially in hot seasons at lower and middle altitudes, where there is the highest water demand, is expected in the near future. Many studies have defined droughts as "a lack of rainfall" based on precipitation data to monitor them (Hao and Aghakouchak, 2013; Jain et al, 2015; Kundu et al, 2020).

It is now evident to experts that a univariate method is not deemed the best for describing droughts' characteristics (Hao and Singh, 2015; Kwon et al, 2019). Droughts constitute multivariate events because any fluctuations of climate variables can increase or decrease their severity (Kundu et al, 2020). Over the years, efforts have been made to develop multivariate indices based on a combination of different drought indices to provide insight into the conditions and characteristics of this event (Svoboda et al, 2002; Beersma and Buishand, 2004; Genest and Favre, 2007; Hao and Aghakouchak, 2014; Li et al., 2015). Various methods and theories have been developed to quantify multivariate indices, such as establishing combinations of precipitation and evapotranspiration variables in different statistical models (Xia et al., 2014), copula functions (Joe, 1997; Nelsen, 2006; Salvadori and Michele, 2007; Hao and Aghakouchak, 2013; Hao and Aghakouchak, 2014; Hao et al., 2014), scalogram model (Ghabaei Sough and Mosaedi 2013, Ghabaei Sough et al 2018), PCA (Principal Component Analysis) (Meyer et al., 1991 Keyantash and Dracup, 2004; Rajsekhar et al., 2014), entropy theory (Hao and Singh, 2015), Markov chain method (Rezaeianzadeh et al., 2019).

The PCA method is a feature extraction and information compression method with a long history in linear algebra and vector analysis (Ghabaei Sough et al., 2018). By the mathematical formulation of the approach, it is completely pliable to develop an aggregate drought index (ADI) from a combination of effective parameters on meteorological, agricultural, and hydrological indices to monitor droughts comprehensively. The studies reported that the ADI structure provides a clear and purposeful way to describe the severity of droughts and can be used easily to express their characteristics in the actual projects (Yu et al., 2015; Bazrafshan et al., 2014 and Li et al., 2015).

Given that droughts are random and multivariate events, their characteristics (severity and duration) are interdependent, meaning that they do not change independently, and any changes in one variable influence the other ones. Furthermore, the bivariate copula function between two main drought's characteristics (severity and duration) can reveal a significant correlation between them, and the return period of drought events are determined by employing this function (Yusof et al, 2013). Kwak et al. (2015) tried to study the impact of climate change on future hydrological droughts. The copula method was applied to analyze the joint probability distribution of droughts. Azam et al. (2018) estimated the values of the four identified homogeneous regions by combining important drought variables (duration and severity) based on the standard precipitation index (SPI). The regional frequency analysis of droughts was conducted by evaluating the probability distributions and copulas. The Pearson type III and Kappa marginal distributions simulated the regional drought variables better. Bivariate stochastic simulation of selected copulas illustrated that the behavior of simulated data may change when the correlation between drought characteristics was considered so the joint distributions were used to estimate conditional probabilities.

In this study, drought conditions due to climate change in the Kamal-Saleh dam basin in Markazi province, Iran, is projected by adopting a new aggregate drought index (ADI) which has calculated by PCA method from two different types of meteorological and hydrological drought index simultaneously for the present and future periods. Most previous research has focused on the drought index separately or has utilized different multi-index without using copula function for drought analysis. Therefore, developing a hydro-meteorological index with minimum climatic parameters and estimating the joint probability distribution and return periods of drought severity and duration by applying the bivariate copula method, successfully has monitored future drought events in the study region and differentiate this study from prior related research.

## **2 Study Area and Data**

This research is conducted on Kamal-Saleh dam basin, one of the most important water supplies in Markazi province, Iran (Fig. 1). It is located southwest of the Markazi province and northeastern of Lorestan province, between  $49^{\circ} 04' 02''$  to  $49^{\circ} 27' 11''$  E and  $33^{\circ} 33' 13''$  to  $33^{\circ} 55' 55''$  N, with a catchment area of  $699 \text{ km}^2$ . The maximum, minimum and average height of the basin is 2960 m, 1840 m and 9490 m, respectively. Since the Markazi province is located in the arid and semi-arid regions of the country, therefore it has always been at the risk of drought and prone to the perceptible impact of climate change on water resources.

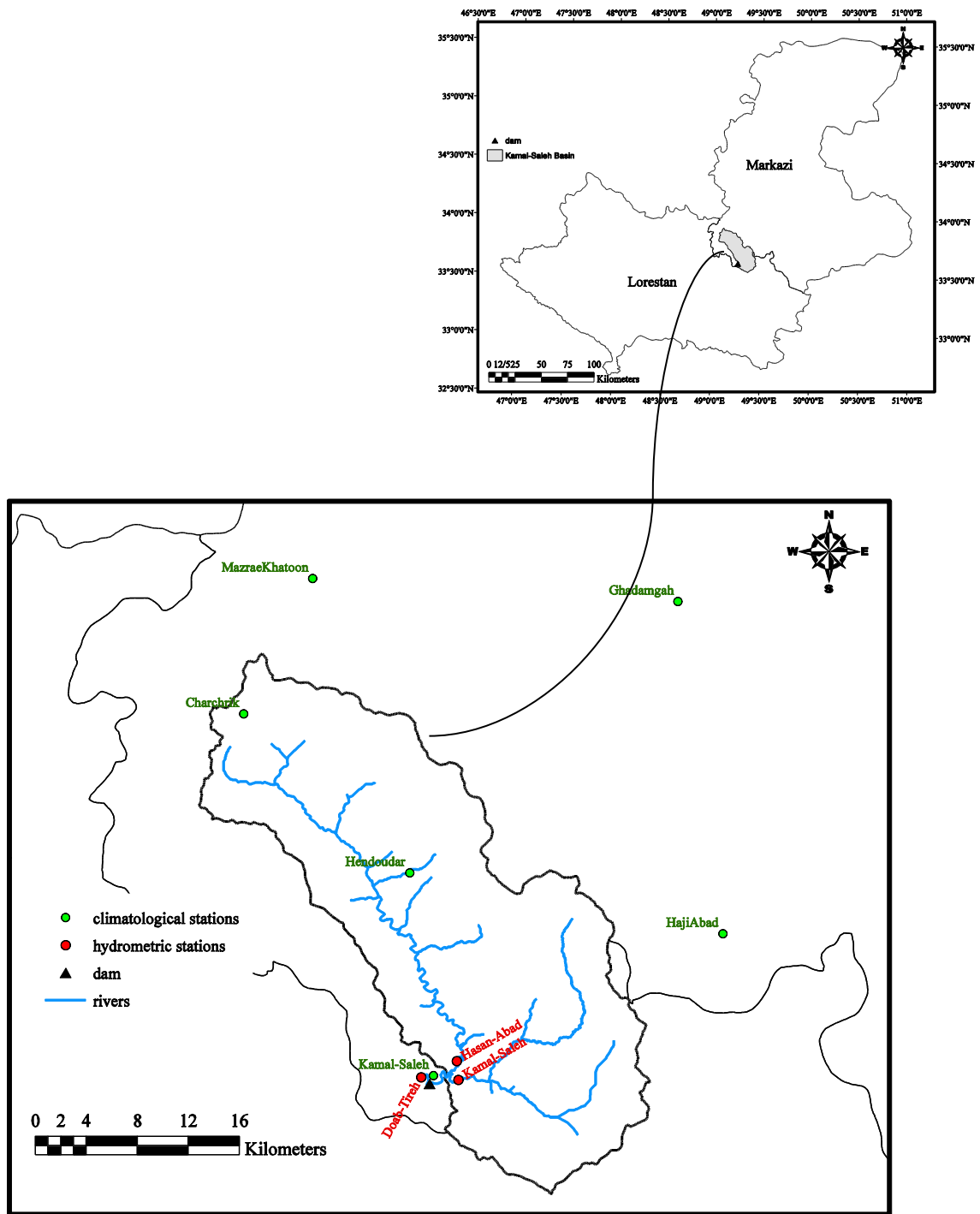


Fig. 1. The study basin and stations

The observed necessary data for this research including daily temperature, precipitation, and monthly streamflow data from 1976 to 2005 is retrieved from the stations located at the Kamal-Saleh basin, shown in Fig. 1. Climate variables on temperature and precipitation in future periods 2050s (2040-2069) and 2080s (2070-2099) are simulated using GCMs under RCP scenarios. The RCP scenarios are consistent with a wide range of possible changes in future anthropogenic (i.e., human) greenhouse gas (GHG) emissions, considering the atmospheric concentrations. In this study two types of these scenarios were adopted:

- RCP4.5: stabilization without overshoot pathway to  $4.5 \text{ W/m}^2$  at stabilization after 2100.
- RCP8.5: rising radiative forcing pathway leading to  $8.5 \text{ W/m}^2$  in 2100. (IPCC, 2014)

The results were then downscaled by SDSM for the study basin. To investigate the impact of climate change on the inflow to Kamal-Saleh dam reservoir, the IHACRES rainfall–runoff model which is a monthly conceptual model was applied. This provides a framework with minimum required parameters which reduces the uncertainties inherent in parameter estimation.

### **3 Methodology**

#### **3.1 SPI, SDI and ADI Indices**

The ADI method provides a clear, objective approach for describing the intensity of droughts. This index is appropriately able to represent the hydro-meteorological drought behavior and is recommended as an integrated index for assessing and monitoring of droughts. Keyantash and Dracup (2004) proposed the flowchart for processing the index on a monthly scale. For this purpose, the monthly values of SPI and Stream flow drought index (SDI) are calculated by Eq. (1)

and Eq. (2) for each time series, and values of the indices are then adjusted for each month in different years in the form of a matrix with specified dimensions (number of months in 2 indices used). The SPI has been developed by McKee et al. (1993) and many drought researchers have acknowledged the flexibility of the SPI and its ability to monitor different aspects of drought (McKee et al, 1993, Haydes et al, 1998, Loukas and Vasiliades, 2005). According to this indicator, the drought occurs when the SPI takes negative values and ends when the SPI becomes positive.

The SPI is calculated as:

$$SPI_n = \frac{[P_0 + \sum(P_{-i}) - \mu_n]}{\delta_n} \quad (1)$$

where:

$n$  = the number of months for which cumulative rainfall is calculated;

$P_0$  = normalized precipitation for the current month;

$P_{-i}$  = normalized precipitation for the last month;

$\mu_n$  = average cumulative precipitation for  $n$  months; and

$\delta_n$  = standard deviation of precipitation for  $n$  months.

SDI calculated from river discharge data can provide a good estimate of hydrological droughts.

The SDI index can be formulated as follows (Nalbantis and Tsakiris, 2009):

$$SDI_{i,k} = \frac{V_{i,k} - \bar{V}_k}{S_k} \quad (2)$$

$V_{i,k}$  = runoff value for  $i$ th month and  $K$ th scale,  $\bar{V}_k$  = average runoff for  $k^{th}$  scale,  $S_k$  = deviation for  $k$ th scale.

One of the most common tools to reduce a data set involving a large number of variables to a new smaller data set is PCA (Wilks, 2011). According to this multivariate statistical technique, the eigenvectors are computed for each set of indices arranged in a matrix. The principal component values were then estimated from linear combination of the input indices for each month and the values of the ADI were calculated. The PCA can be employed to distill the critical information from available different kind of drought-related variables or indices. According to this concept, ADI as a multivariate drought index is formed that includes all physical forms of drought, such as hydrological and meteorological drought (Keyantash and Dracup, 2004; Hao and Singh, 2015). By the PCA method the ADI is the first principal component that it normalized via monthly time series of standard deviation. Since the ADI is a standardized index, it follows the same drought classification criterion of SPI, so that the drought event is considered to be ongoing until the ADI is continuously negative and becomes -1 or less and end when ADI is positive. It should be noted that for some drought events, although the SPI value has never been lower than -1, due to the long duration of these events, their cumulative amount and effect is greater than other droughts which SPI is less than -1.

Acute problems of water resources during the drought period are generally related to such long-term events. In this study, according to the recommendation of Lucas and Vasiliades (2004), the drought event is defined as a period that the SPI values and consequently the ADI values are less than zero. Therefore, positive values of ADI indicate overall wet conditions, while negative and zero values suggest overall dry and normal conditions, respectively.

In order to define drought characteristics, Run theory has used. Based on Run theory with reference to Fig. 2, the drought severity (S) is expressed as the sum of the negative values of the index over the continuous period of drought, which can be calculated as follows:

$$S = -\sum_{i=1}^D index_i \quad (3)$$

The drought duration (D) is expressed as the duration of continuous drought.

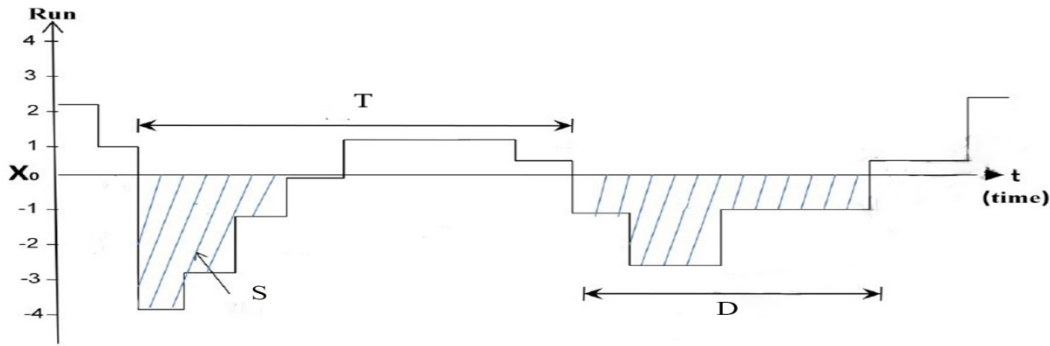


**Fig. 2.** Definition sketch of drought characteristics showing two drought events (Yevjevich and Ingenieur, 1967)

### 3.2 Selection of appropriate marginal distribution

The classical study by Sklar in 1959 had the imperative results pertaining to this topic by introducing the notion and the name of a copula, and proving the theorem that now bears his name. From another attitude, copulas are functions that join or “couple” multivariate distribution functions to their one-dimensional marginal distribution functions. Alternatively, copulas are multivariate distribution functions whose one-dimensional margins are uniform on the interval (0, 1) (Nelsen, 2006).

The study uses bivariate copula functions to create a severity-duration bivariate distribution. So technically, the copula approach divides the problem into two mutually independent steps concerning fitting the marginal distributions and finding the dependence structure among the margins (Nazemi & Elshorbagy, 2012). In this study, five univariate distribution functions have fitted to the severity and drought observation data using the Kolmogorov-Smirnov test. The

distribution functions adopted in this research are listed in Table 1. The estimation method for the parameter of marginal distributions is the maximum likelihood method, and the Kolmogorov–Smirnov (K-S) test method evaluates the fitting degree (Laio, 2004). The Maximum likelihood estimation (MLE) estimates the parameters of  $f(x)$ . Next, proper copula functions are needed to integrate both D and S.

**Table 1.** Distribution functions and their Cumulative Distribution Function

Type	Cumulative Distribution Function (CDF)
Exponential	$f(x) = \lambda e^{-\lambda x}$
Gamma	$f(x) = \frac{\beta^\alpha x^{\alpha-1} e^{-x/\beta}}{\Gamma(\alpha)}$
Normal	$f(x) = \frac{1}{\sigma\sqrt{2\pi}} e^{-\frac{(x-\mu)^2}{2\sigma^2}}$
Lognormal	$f(x) = \frac{1}{x\sigma\sqrt{2\pi}} e^{-\frac{(\ln x - \mu)^2}{2\sigma^2}}$
Weibull	$f(x) = \begin{cases} \frac{\alpha}{\beta} \left(\frac{x}{\beta}\right)^{\alpha-1} e^{-x/\beta}, & x = 0 \\ 0, & x \neq 0 \end{cases}$

### 3.3 Copula functions

In this study, five bivariate copula functions, including Clayton, Frank, Gumbel, Joe and Guassian have been considered to fit the marginal distributions and to create the joint probability of drought severity and duration. Estimating the parameter of the copula functions is needed to fit these functions to drought duration and severity. There are several methods to estimate the joint

dependence parameter on the data. In this study, the parameter is estimated by the log-likelihood function. In the selection of best-fitted Copula, the optimal Copula was elected based on maximizing the log-likelihood function of the copula model (Nelsen, 2006). Copula families adopted in this research are listed in Table 2.

**Table 2.** Investigated copula functions in the present study

Copula type	Cumulative Distribution Function, $c(u, v)$	Parameter Range
Clayton	$(u^{-\theta} + v^{-\theta} - 1)^{-1/\theta}$	$\theta \geq 0$
Frank	$-\frac{1}{\theta} \ln \left[ 1 + \frac{(e^{-\theta u} - 1)(e^{-\theta v} - 1)}{e^{-\theta} - 1} \right]$	$\theta \neq 0$
Joe	$1 - [(1-u)^\theta + (1-v)^\theta - (1-u)^\theta + (1-v)^\theta]^{1/\theta}$	$\theta \geq 0$
Gumball	$\exp \left\{ - [(-\ln u)^\theta + (-\ln v)^\theta]^{1/\theta} \right\}$	$\theta \geq 1$
Gaussian	$\Phi_2(\Phi^{-1}(u), \Phi^{-1}(v), \rho)$	$-1 \leq \rho \leq 1$

### 3.4 Joint probabilities of droughts

The probability that both severity and drought characteristics exceed a certain threshold provides useful information to improve the water resources management under drought conditions. This probability cannot be calculated through a univariate analysis of severity and duration of drought, whereas it can be easily obtained by the copula functions (Shiau, 2006). The joint distribution function of drought duration and severity is defined by Copula function:

$$P(D \geq d, S \geq s) = 1 - F_D(d) - F_S(s) + C(F_D(d), F_S(s)) \quad (4)$$

Where  $P(D \geq d, S \geq s)$  is the probability that both severity (S) and drought duration (D) exceed a certain threshold.  $F_d(D)$  and  $F_s(s)$  are the cumulative drought duration and severity distribution functions and  $C(F_d(D), F_s(s))$  introduces the copula function. Duration and severity are two characters that describe droughts as bivariate events.

### 3.5 Correlation analysis of variables

There are several methods to investigate the correlation among drought characteristics. The dependence measures can be assessed using Pearson's linear correlation  $r$ , Spearman's rank correlation  $\rho$ , and Kendall's  $\tau$  (for more details, refer to Chen and Guo (2019)).

### 3.6 Bivariate drought return period

Planning and managing water resources systems under drought conditions need estimations based on the return period of drought (Kim et al, 2003). Shiau and Shen (2001) theoretically derived the return period for droughts with severity greater than or equal to a certain value,  $s'$ , as a function of the expected drought inter-arrival time and cumulative drought severity distribution function, expressed as:

$$T_s = \frac{E(L)}{1 - F_s(S')} \quad (5)$$

Where  $L$  is the drought inter-arrival time;  $E(L)$  is the expected drought inter-arrival time, which can be estimated from observed droughts; and  $T_s$  is the return period defined solely by the drought severity. Similarly, the return period for drought duration greater than or equal to a certain value,  $d'$ , can be written as:

$$T_D = \frac{E(L)}{1 - F_D(d')} \quad (6)$$

where  $T_D$  is the return period defined only by the drought duration.

Droughts are considered bivariate events characterized by drought duration and severity. Shiau (2006) proposed a methodology that categorizes the return periods of bivariate distributed hydrologic events as joint and conditional return periods. According to the joint probability distribution of droughts, return periods for  $D \geq d$  and  $S \geq s$  as  $T_{DS}$  and return period for  $D \geq d$  or  $S \geq s$  as  $T'_{DS}$  are defined for base and future periods where  $F_D(d)$  and  $F_S(s)$  are the cumulative distribution functions of drought duration and severity,  $C$  is the copula function and  $E(L)$  is the average inter-arrival time.

$$T_{DS} = \frac{E(L)}{P(D \geq d, S \geq s)} = \frac{E(L)}{1 - F_D(d) - F_S(s) + C(F_D(d), F_S(s))} \quad (7)$$

$$T'_{DS} = \frac{E(L)}{P(D \geq d \text{ or } S \geq s)} = \frac{E(L)}{1 - C(F_D(d), F_S(s))} \quad (8)$$

### 3.7 Conditional return period

Similarly, the conditional return period can be prepared for two cases: (a)  $T_{D|S \geq s'}$  (b)  $T_{S|D \geq d'}$

These conditional return periods are obtained as follows (Yusof et al, 2013):

$$T_{D|S \geq s'} = \frac{T_S}{P(D \geq d, S \geq s)} = \frac{E_L}{[1 - F_S(s)][1 - F_D(d) - F_S(s) + C(F_D(d), F_S(s))]} \quad (9)$$

$$T_{S|D \geq d'} = \frac{T_D}{P(D \geq d, S \geq s)} = \frac{E_L}{[1 - F_D(d)][1 - F_S(s) - F_D(d) + C(F_D(d), F_S(s))]} \quad (10)$$

where,  $T_{D|S \geq s'}$  is conditional return period for drought duration, D, while  $S \geq s'$  and  $T_{S|D \geq d'}$  is conditional return period for drought severity, S, while  $D \geq d'$ . The parameters  $d'$  and  $s'$  are specific values of duration and severity, respectively.

## 4 Result and discussion

### 4.1 Selecting the best GCM for Kamal-Saleh dam basin

In this study, a suitable GCM for the region is selected by hindcast approach whereby the performance of GCMs are evaluated through comparison of historical model simulations with observations (Farjad et al., 2019). Five of the most widely used GCMs were initially selected and evaluated by the hindcast approach (Table 3 and Fig. 3). Also, to assess the performance of GCMs, the coefficient of correlation (R), root mean square error coefficient (RMSE) and mean absolute error (MAE) were applied. Based on the model comparison approach, CanESM2 was determined as one of the best performance model compared to other GCMs in the region studied.

**Table 3.** Assessing the performance of some GCMs in the study region

Variable		FGOAL	GMCC-CM	NorESM	CNRM	<b>CanESM2</b>
Temperature	RMSE (°C)	0.33	1.01	0.73	0.9	<b>1.3</b>
	MAE (°C)	2	3.2	2.7	2.4	<b>4.5</b>
	R (%)	99	98	99	99	<b>85</b>
Precipitation	RMSE (mm)	30.6	10.3	14.6	17.1	<b>12.3</b>
	MAE (mm)	0.75	1.00	0.66	1.2	<b>0.65</b>
	R (%)	47	95	93	88	<b>95</b>

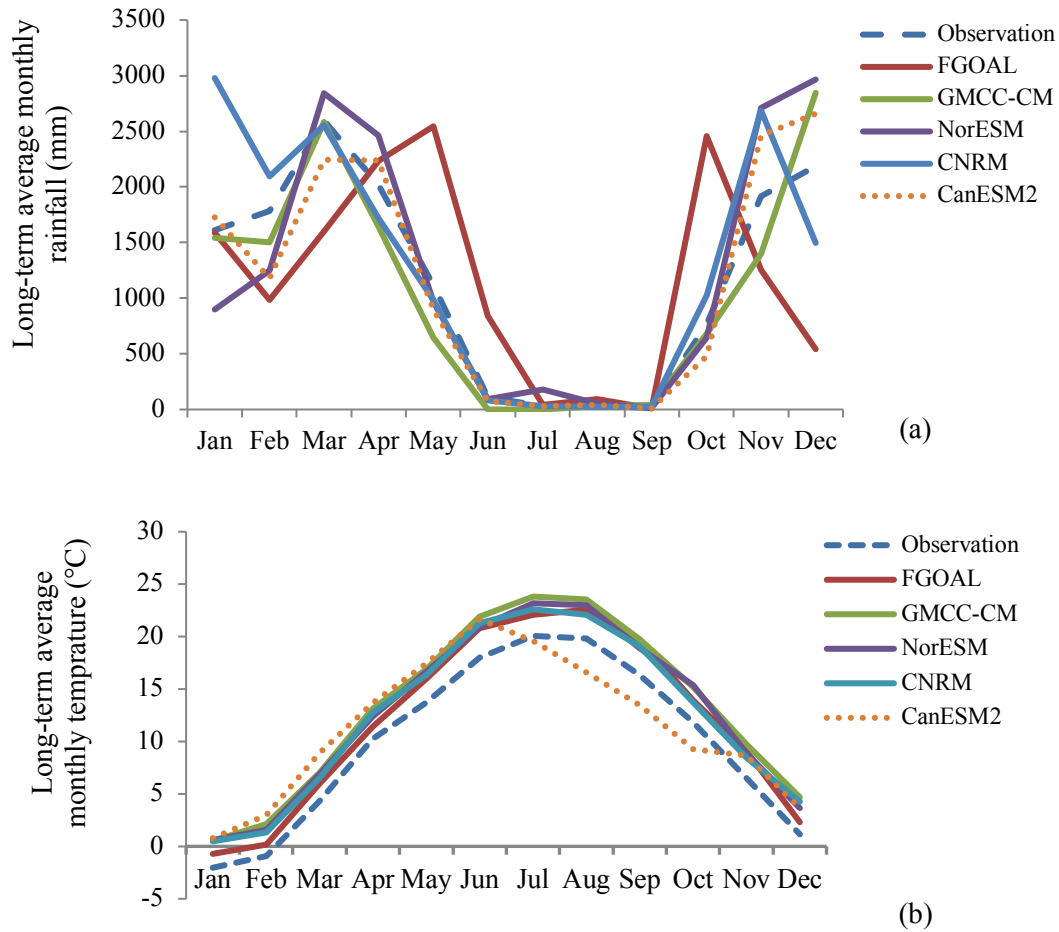


**Fig. 3.** Comparison of long-term average of monthly rainfall and temperature values in the base period: (a) rainfall  
(b) temperature

#### 4.2 Calculation of drought indices

The hydrological index (SDI) and meteorological index (SPI) are calculated on the monthly scale. The values of the indices are shown in Fig. 4 for the base period. As this figure illustrates, although these two indices are generally consistent, there are differences between them over several time intervals. One of the reasons for this difference could be the fundamental role of temperature in the rate of evaporation and transpiration in this semi-arid region. This is probably because a sizable portion of rainfall is lost as water vapor to the atmosphere by evaporation and transpiration, which

greatly impacts on the rate of runoff and subsequently leads to hydrological drought. Another reason is likely due to the abnormally heavy rainfall in a very short time, while most of the month is dry (SPI > 0 and SDI < 0).

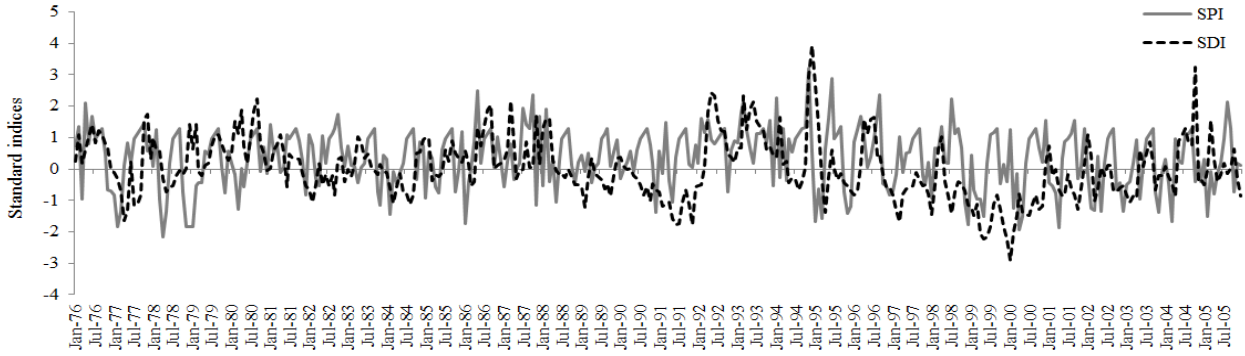


**Fig. 4.** The monthly SPI and SDI (base period) for region studied

ADI is calculated by the PCA method described in section 3-1. The following steps summarize the calculation of this index for the base period.

Initially the matrix X is created as its rows indicate the months in the base period and the columns show associated SPI and SDI values:

$$X = \begin{matrix} \text{Jan - 1976} \\ \text{Feb - 1976} \\ \text{Mar - 1976} \\ \vdots \\ \text{Oct - 2005} \\ \text{Nov - 2005} \\ \text{Dec - 2005} \end{matrix} \begin{bmatrix} \text{SPI} & \text{SDI} \\ 0.731361 & 0.247625 \\ 1.360323 & 1.076231 \\ -0.95672 & 0.170052 \\ \vdots & \vdots \\ -0.72765 & 0.634189 \\ 0.187308 & -0.29355 \\ 0.126685 & -0.85629 \end{bmatrix}$$

Computation of the main component of the PCA requires the production of a symmetric square matrix (R) to describe the relationship between the main data. R is the correlation matrix between

SPI and SDI (Eq. 11). Here, N is the number of months in the 30-year period (360 months) and  $X^T$  is the transpose of the matrix.

$$R = \frac{1}{N-1} \times X^T \times X = \begin{bmatrix} 1.0286 & 0.1557 \\ 0.1557 & 0.9417 \end{bmatrix} \quad (11)$$

eigenvector array for this time series is determined as:

$$e_1 = [u, R] = \text{eig}(R) = [0.6047 \quad -0.7965] \quad (12)$$

Subsequently, ADI is defined as Eq. (13) where  $\sigma$  is the principal component's standard deviation.

$$ADI = \frac{1}{\sigma} \times X \times e_1 = \frac{1}{0.88378} \times \begin{bmatrix} 0.731361 & 0.247625 \\ 1.360323 & 1.076231 \\ -0.95672 & 0.170052 \\ \cdot & \cdot \\ \cdot & \cdot \\ \cdot & \cdot \\ \cdot & \cdot \\ -0.72765 & 0.634189 \\ 0.187308 & -0.29355 \\ 0.126685 & -0.85629 \end{bmatrix} \quad (13)$$

Fig. 5 shows the ADI values in the base period for the region studied. According to Fig. 5, the historical values of the ADI vary from -3.5 to 3.5. The most severe drought is obtained in January 1995 and October 2004, also the longest duration are 11, 10 and 7 months which would occur from May to March 1976, January to October 1980, April to October 1992 and March to September 1993, respectively. Figs. 6 and 7 show ADI values for the two future periods (2050s and 2080s) under two RCP scenarios. According to Fig. 6, drought index values reveal more fluctuation in the first 30-year period, and this period would have droughts with longer durations relative to another period. Although in the second 30-year period, the ADI values are in a larger interval, the peak points of drought are greater. So more severe droughts with shorter durations will be seen in the far future compare to the near future. Despite the result of Fig. 6, Fig. 7 shows that the first period

would deal with more severe and longer drought in comparison with the second period in the future under RCP8.5 but like RCP4.5 peak points in the second period show higher values.

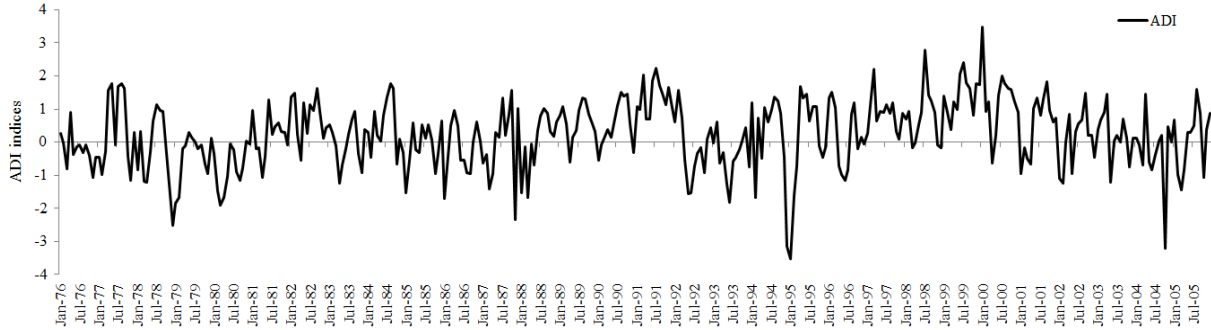


Fig. 5. The monthly ADI (base period)

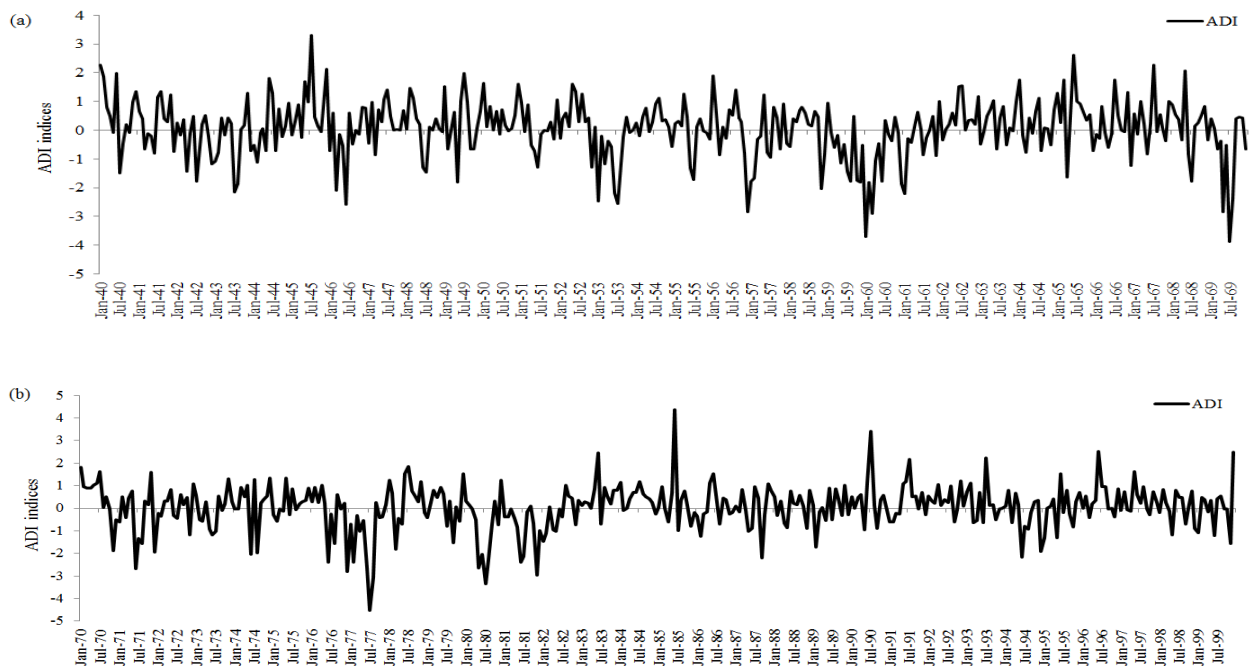
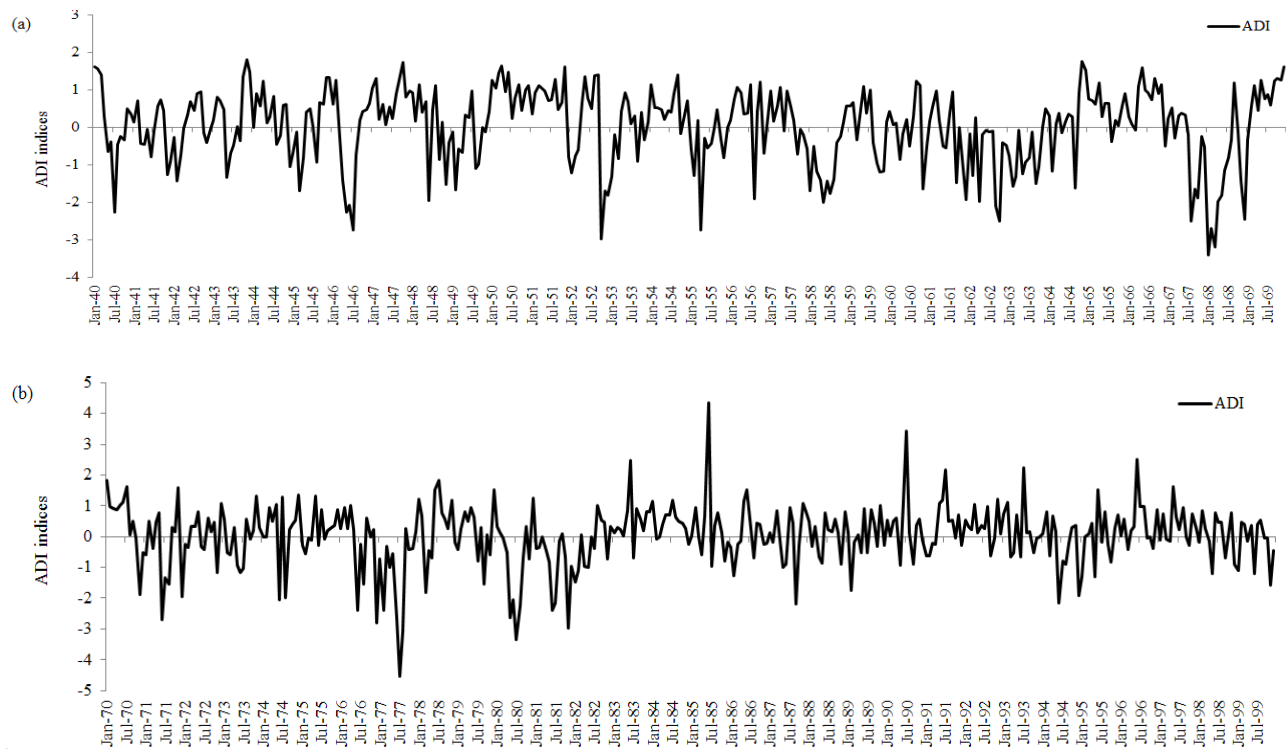


Fig. 6. Comparison of ADI for two future periods under RCP4.5 (a) 2050s (b) 2080s



**Fig. 7.** Comparison of ADI for two future period under RCP8.5 (a) 2050s (b) 2080s

### 4.3 Investigation correlation between drought duration and severity

The hydro-meteorological drought severity and duration data are extracted from Figs. 6 and 7 based on the runs theory as shown in Fig. 2. The summary description of drought events and characteristics for each scenario and time series are prepared in Table 4.

**Table 4.** The summary description of drought events and characteristics for each time series and scenarios

		Base period	RCP4.5		RCP8.5	
			2050s	2080s	2050s	2080s
The number of drought events		55	79	77	44	77
Drought duration	Minimum	1	1	1	1	1
	Maximum	11	10	10	19	8
	Standard Deviation	2.28	2	2.06	3.5	2.01
	Mean	2.6	2.65	1.73	3.88	1.53
Drought severity	Minimum	0.0026	0.0064	0.0174	0.0093	0.0174
	Maximum	9.52	15.88	18.03	22.41	25
	Standard Deviation	2.21	2.01	1.64	3.19	1.63
	Mean	1.92	1.84	2.65	4.67	2.65

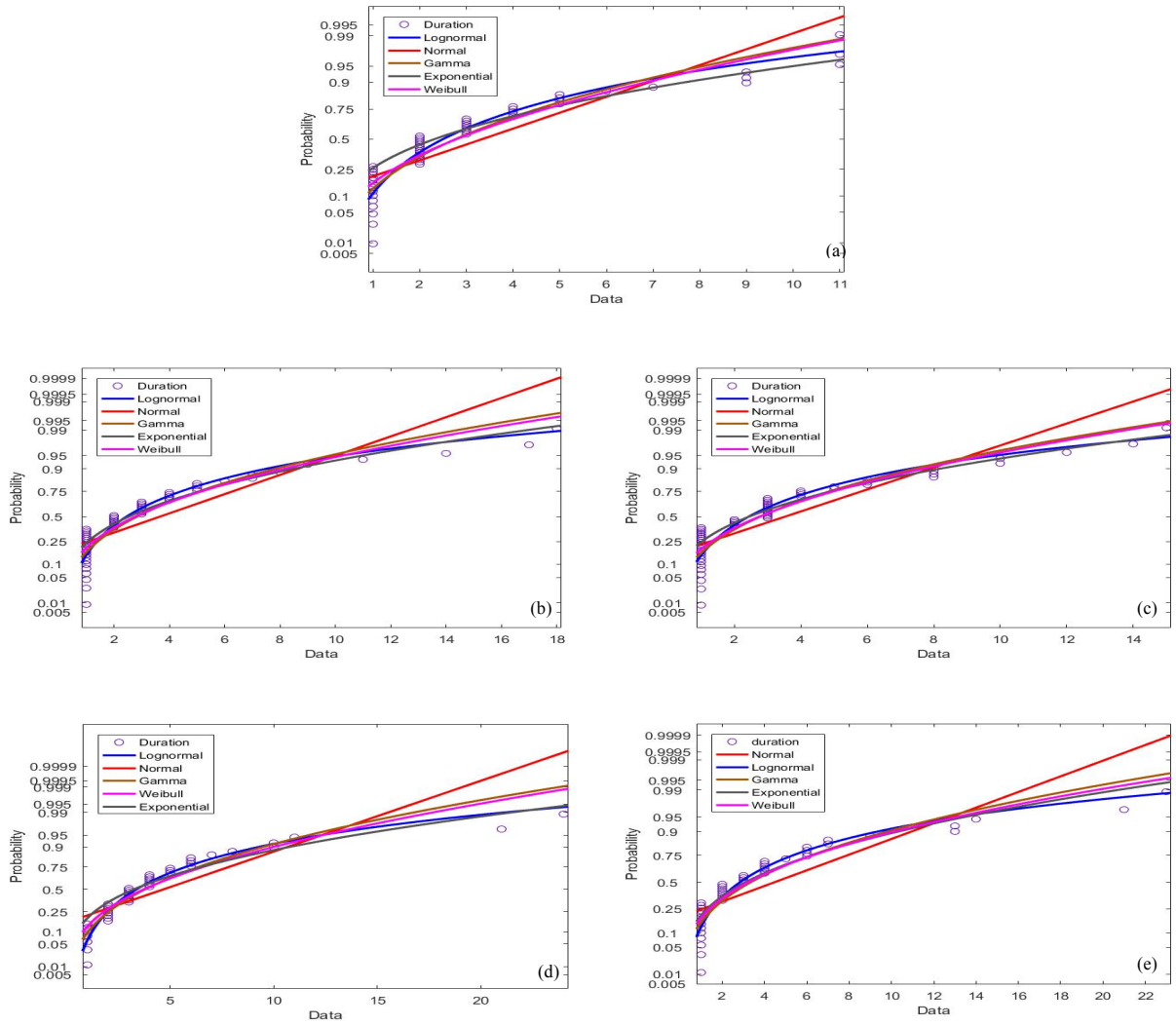
Correlation metrics such as Pearson, Kendall's tau, and Spearman's rho are computed and prepared in Table 5. Pearson's correlation coefficient considers only the linear correlation between the data and in the presence of severe dependencies, this coefficient may not be computable. Non-parametric correlation coefficients such as Spearman and Kendall Tau coefficients may overcome the defect of the Pearson coefficient (Salvadori and Michele, 2007). Before the joint distribution function has established, these three rank correlation coefficients are also adopted to test the correlation between drought duration and severity. The results show that there is a positive correlation between the drought severity and duration variables based on three methods that are used.

**Table 5.** Correlation between drought severity and duration for each time series and scenarios

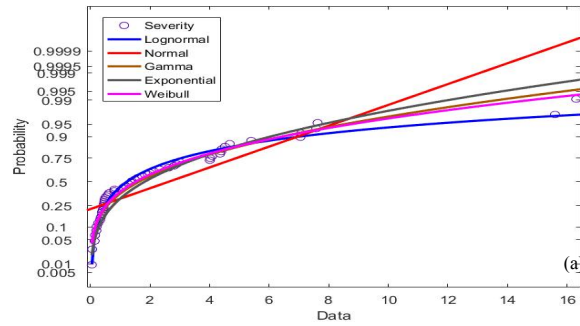
	Base period	RCP4.5		RCP8.5	
		2050s	2080s	2050s	2080s
Pearson	0.82	0.88	0.85	0.93	0.74
Kendall's tau	0.63	0.58	0.54	0.74	0.54
Spearman	0.76	0.71	0.68	0.86	0.67

#### 4.4 Estimation of marginal distributions for drought duration and severity

Following the recommendations of Ayantobo et al. (2017) in the selection of marginal distributions, the drought duration (D) and severity (S) fitted with their corresponding marginal distributions. The results have been illustrated in Figs. 8 and 9. It can be seen that the lognormal fits the drought duration and severity well for all of the time series and scenarios.



**Fig. 8.** Comparison between the best-fitted marginal distributions for drought duration (a) base period, (b) 2050s under RCP4.5, (c) 2080s under RCP4.5, (d) 2050s under RCP8.5, (e) 2080s under RCP8.5



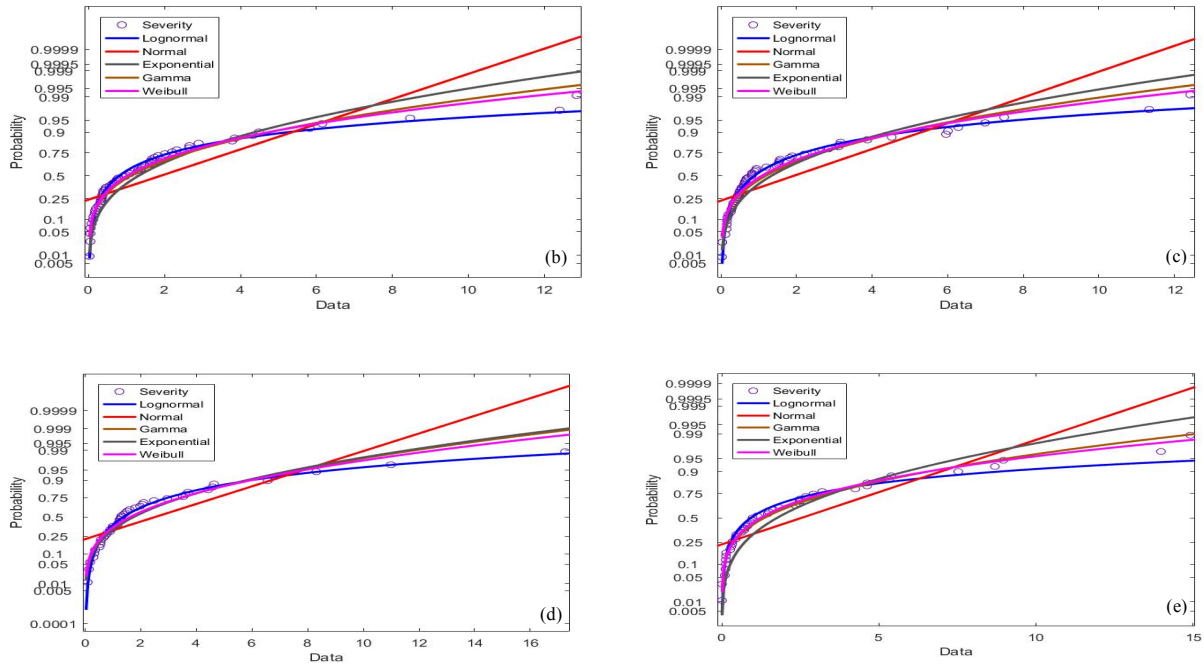


**Fig. 9.** Comparison between the best-fitted marginal distributions for drought severity (a) base period, (b) 2050s under RCP4.5, (c) 2080s under RCP4.5, (d) 2050s under RCP8.5, (e) 2080s under RCP8.5

The parameters of these distributions are estimated by the maximum likelihood method for the base and the two future periods (Table 6). The results illustrate that the lognormal well-fits the drought duration and severity for all-time series and scenarios. Therefore, lognormal function as the optimal distribution function is selected and its parameters are shown in Table 7.

**Table 6.** The maximum likelihood function of marginal distribution functions

Type	Base period		2050s				2080s			
			RCP4.5		RCP8.5		RCP4.5		RCP8.5	
	D	S	D	S	D	S	D	S	D	S
Normal	-122.91	121.312	-161.08	-188.66	-121.65	-150.43	-150.83	-183.82	-141.73	-183.83
<b>Log-Normal</b>	<b>-96.67</b>	<b>-96.83</b>	<b>-110.87</b>	<b>-104.19</b>	<b>-93.05</b>	<b>-92.1</b>	<b>-110.92</b>	<b>-132.9</b>	<b>-119.39</b>	<b>-115.22</b>
Gamma	-128	-247.34	-124.46	-281.25	-339.41	-645.1	-126.08	-239.49	-186.27	-239.49
Exponential	-319/24	-167.12	-261.24	-162.34	-483.88	-397.21	-272.49	-168.99	-258.14	-167
Weibull	-1411.36	-382.46	-381.43	-229.53	-58651.4	-16678.8	-348.42	-278.73	-242.15	-278.73

**Table7.** Estimated Parameters for optimal marginal (lognormal) distribution

Time series		Parameter	
		D	S
Base period		$\alpha= 0.67$	$\alpha= -0.16$
		$\beta= 0.73$	$\beta= 1.67$
2050s	RCP4.5	$\alpha= 0.44$	$\alpha= -0.51$
		$\beta= 0.63$	$\beta= 1.51$
	RCP8.5	$\alpha= 0.82$	$\alpha= 0.25$
		$\beta= 0.89$	$\beta= 1.55$
2080s	RCP4.5	$\alpha= 0.44$	$\alpha= 0.51$
		$\beta= 0.67$	$\beta= 2.65$
	RCP8.5	$\alpha= 0.82$	$\alpha= -0.077$
		$\beta= 0.78$	$\beta= 1.76$

#### 4.5 Analysis of joint distribution functions of drought duration and severity

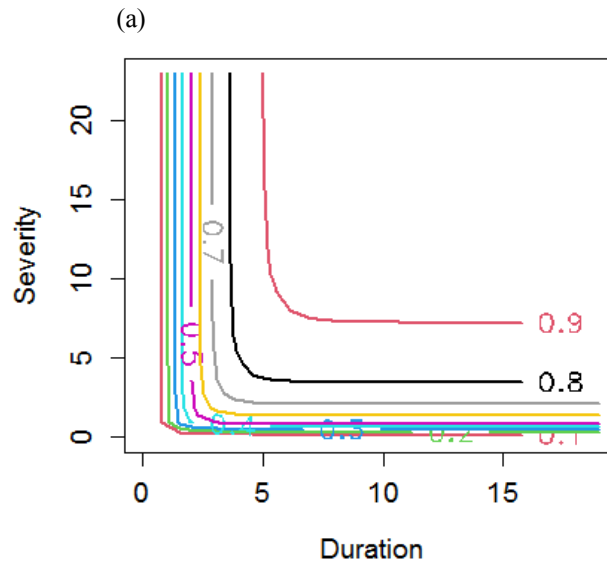
After fitting the optimal marginal distribution function to the drought characteristics, five common copula functions (listed in table 2) are considered to analyze joint distribution functions of drought duration and severity. In order to establish an optimal copula function, copula dependence parameters must be calculated. The maximum likelihood method has been used to calculate the

copula dependence parameters. The AIC and BIC values are also performance criteria that their lower values would imply better fitting. The results of the most optimal copula function in each periods and scenarios and their parameters are presented in Table 8.

**Table 8.** Features of optimal copula functions

	Time series	Optimal copula function	Parameter ( $\Theta$ )	MLE	AIC	BIC
	Base period	Gumbel	2.47	25.83	-49.66	-47.66
RCP4.5	2050s	Clayton	2.16	34.37	-66.74	-64.37
	2080s	Clayton	1.97	30.34	-58.68	-56.33
RCP8.5	2050s	Clayton	3.93	32.29	-62.57	-60.79
	2080s	Clayton	1.78	27.59	-53.18	-50.84

The selected optimal marginal distributions and optimal copula produce the copula-based joint distribution of drought duration and severity. The joint probabilities of drought severity and duration can be seen in Fig. 10. Expectedly, the contours of 0.1 to 0.9 in all cases are different.



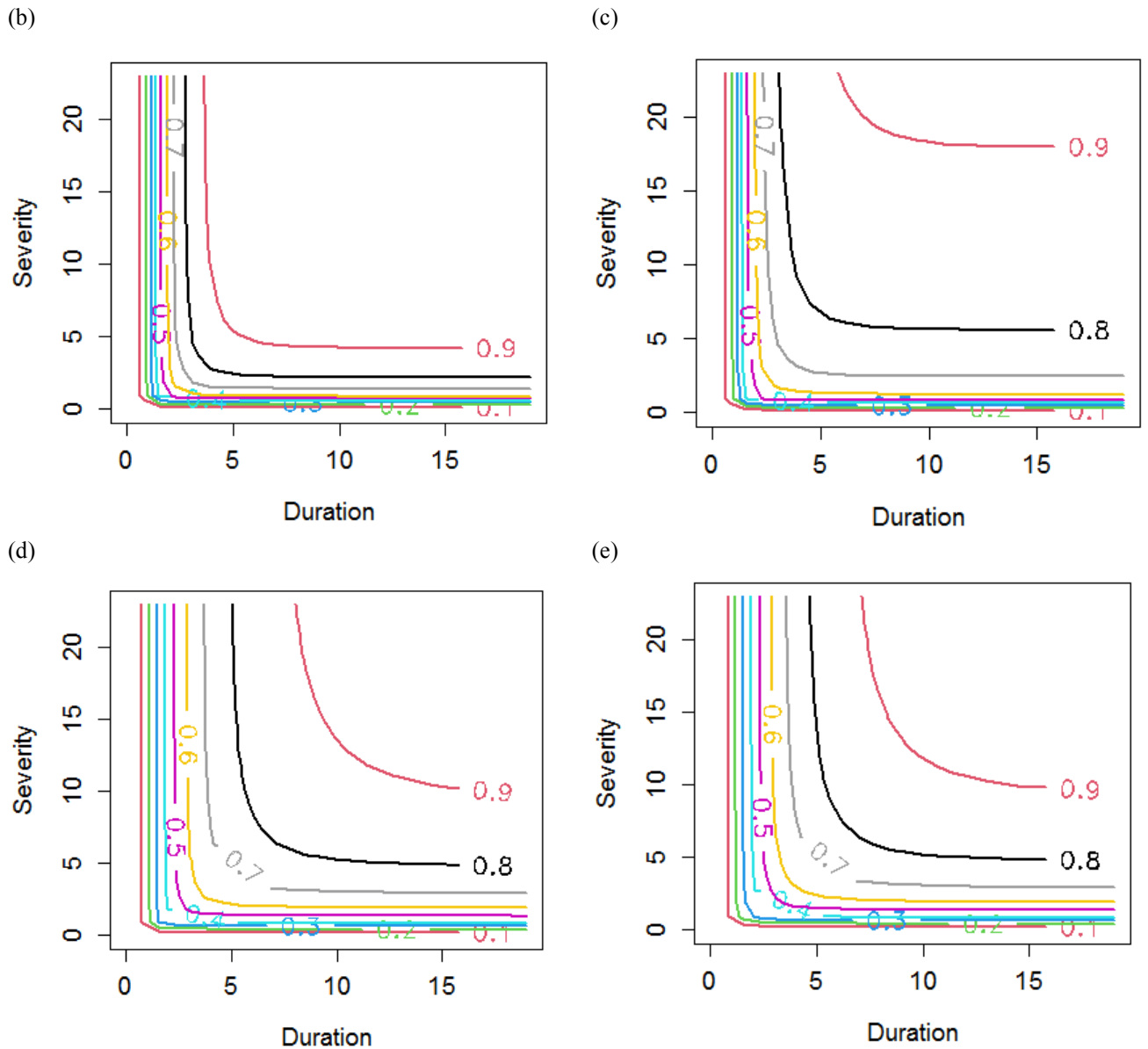


**Fig. 10.** Contours of joint probabilities of drought severity and duration for (a) base period, (b) 2050s under RCP4.5, (c) 2080s under RCP4.5, (d) 2050s under RCP8.5, (e) 2080s under RCP8.5

Fig. 10 enable understanding probabilities of varied different cases of drought severity and duration. For example in Fig. 10.b (2050s under RCP4.5), the plotted contours denoted the

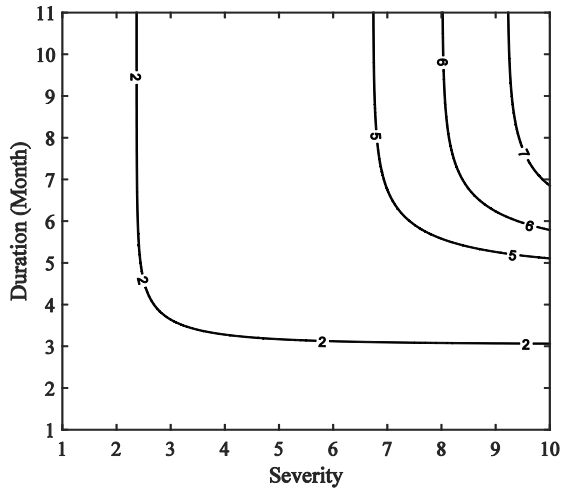
probability of severe drought is less, compared with all others. While in Fig.10.c (2050s under RCP4.5), the probability of occurrence severe and long drought is considerably more than other cases in this study. Also for both future periods, the probability of happening severe drought is more than base period under RCP8.5.

#### **4.6 Bivariate return period of droughts**

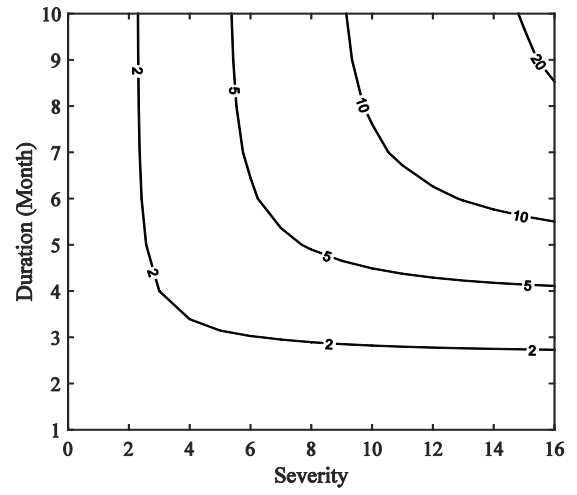
The results of return periods estimated from Eqs. 7 and 8 are shown in Figs. 11 and 12. When a drought occurs with a certain return period, shorter droughts and relatively more severe than the base period are likely to occur for all cases when either duration or severity exceed certain levels. This indicates droughts will occur with a shorter duration and greater severity in the future, especially this increase is more considerable in the second period and the RCP8.5. As a result, the maximum drought return period for  $D \geq d$  or  $S \geq s$  ( $T'_{DS}$ ) in the base period is 7 years, while in future in the years 2050s under RCP4.5 and RCP8.5 scenarios, will be 22 and 17 years respectively, and in the years 2080s under both scenarios will be 3 years (Fig. 11).

Also maximum return period for  $D \geq d$  and  $S \geq s$  ( $T_{DS}$ ) in base period is 62, in the years 2050s under RCP4.5 and RCP8.5 scenarios, will be 4000 and 540 years, respectively and in the years 2080s under RCP4.5 will be 800 and under RCP8.5 will be 57 years (Fig. 12).

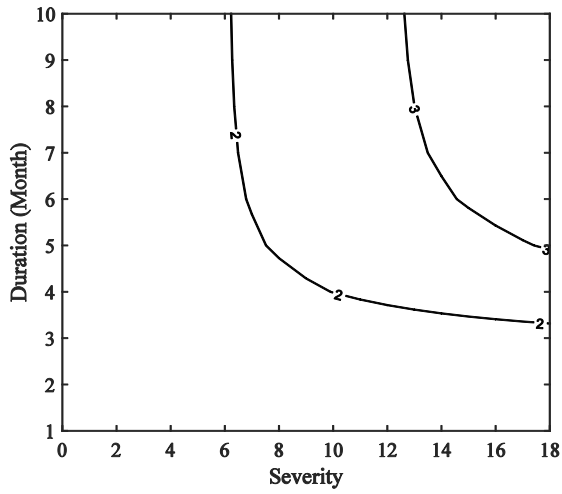
(a)



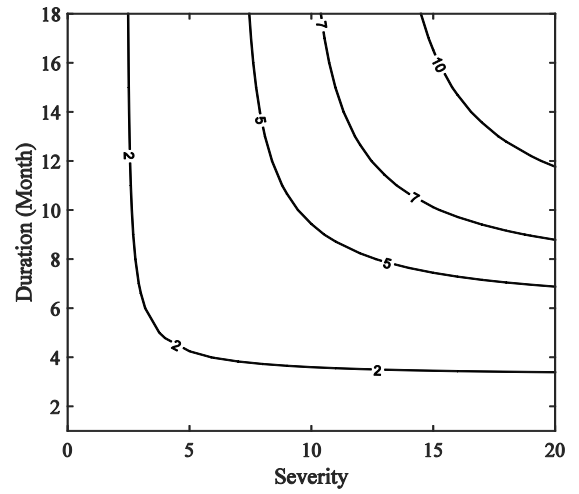
(b)



(c)



(d)



(e)

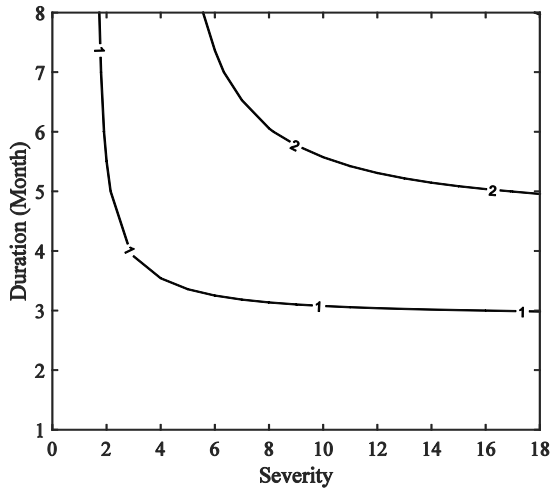
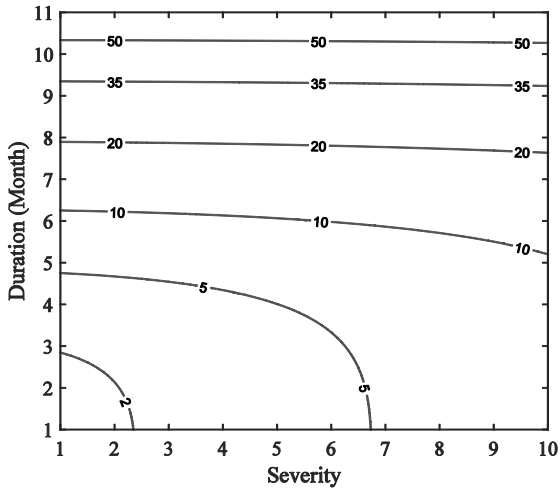
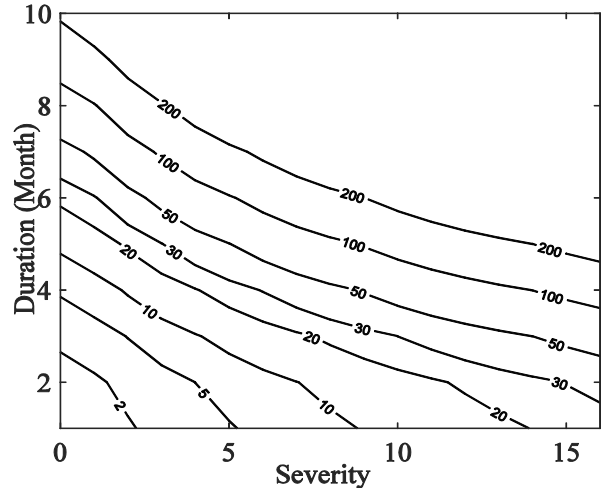


**Fig. 11.** Joint return period of drought duration or severity exceeding certain levels ( $T'_{DS}$ ) for (a) base period, (b) 2050s in RCP4.5, (c) 2080s in RCP4.5, (d) 2050s in RCP8.5, (e) 2080s in RCP8.5

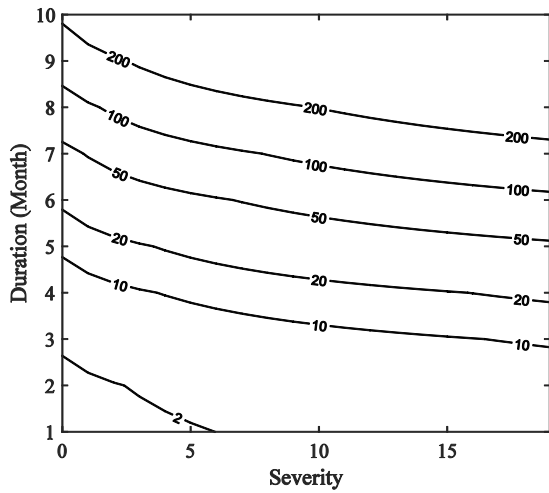
(a)



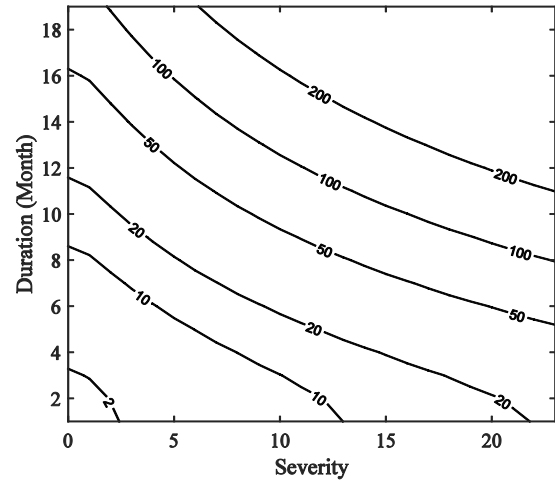
(b)



(c)



(d)



(e)

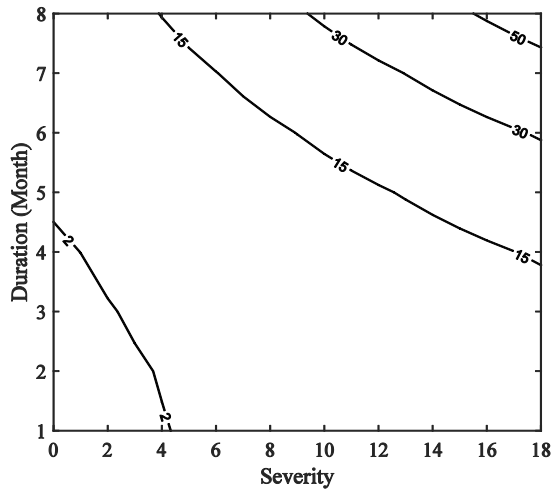


**Fig. 12.** Joint return period of drought duration and severity both exceeding certain levels ( $T_{DS}$ ) for (a) base period, (b) 2050s under RCP4.5, (c) 2080s under RCP4.5, (d) 2050s under RCP8.5, (e) 2080s under RCP8.5

On the other hand, Figs. 11 and 12 illustrate the estimated return period for any given duration and/or severity exceeding a certain level. Under RCP4.5, compared with the base period, the return period will be greater, while for RCP8.5, with a certain return period, droughts will occur with a shorter duration and greater severity in the future. When both variables (severity and duration)

exceeded a certain value, the return period is more extended; for example in historical period, a drought event with a severity of 5 and duration of 7 months, will occur with a return period of approximately 14 years, while the drought with the same severity and duration in the period of 2050s will have a return period of 172 and 11 years under RCP4.5 and RCP8.5 scenarios, respectively. The corresponding values for the period 2080s will be 82 and 13, respectively. Totally, the potential droughts in the future would become more frequent and more severe, except for RCP4.5, which drought will occur with a longer return period for the situation that both duration and severity exceed certain levels.

#### **4.7 Conditional return period**

The conditional return period of drought duration and severity were defined according to Eqs. 9 and 10 for the base period and two future periods under RCP4.5 and RCP 8.5 scenarios and the results are demonstrated in Figs.14 and 15. Conditional return periods can provide valuable information to water resources managers for risk assessment on water resources. It is always necessary to measure a region's water supply system's ability to meet and manage its water needs in certain drought conditions.

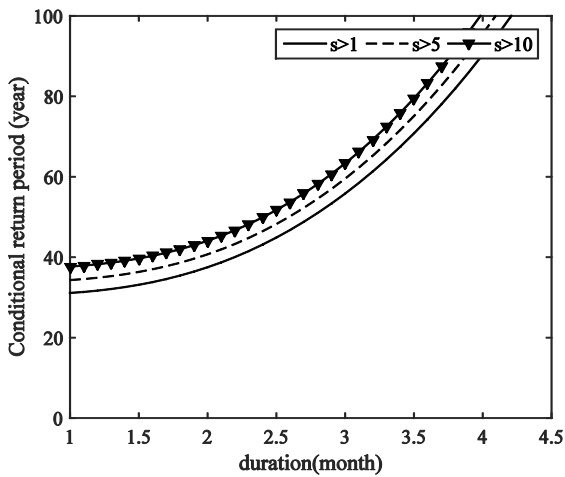
Fig. 13 shows conditional return period of drought duration for a given drought severity ( $s$ ) where  $s$  exceeding the threshold level ( $s'$ ), for instance  $s'=1, 5$  and  $10$ . For example, for a drought severity exceeding an index of 5 during a drought duration more than 3 months, the return period is around 65 years in the historical period while in the period of 2050s, the return period would be about 120 and 40 years under RCP4.5 and RCP8.5 scenarios respectively. These corresponding values would be roughly 90 and 30 years respectively in the 2080s.

For another case, investigating the conditional return period of drought severity which is shown in Fig. 14 indicates for instance when drought duration exceeding 5 months and its severity is greater

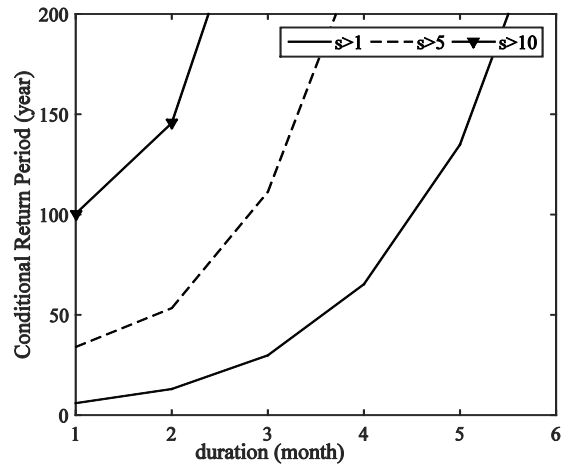
than 3, the return period is approximately 30 years in the historical period while the corresponding values would be about 40 and 37 years in the 2050s and about 22 and 20 years in the 2080s respectively under RCP4.5 and RCP8.5 scenarios.

Although the plots with various  $s'$  values have similar pattern but the results indicate that for a given drought duration, the conditional return period of drought occurrences increases as  $s'$  values increase (Fig. 13). Figure 14 shows similar results. The amount of these increases are more significant in the future periods. Also the results indicate that in future periods, the conditional return periods of a particular duration with a given severity decrease in 2080s compare to 2050s; in addition, those decrease in RCP8.5 compare to RCP4.5.

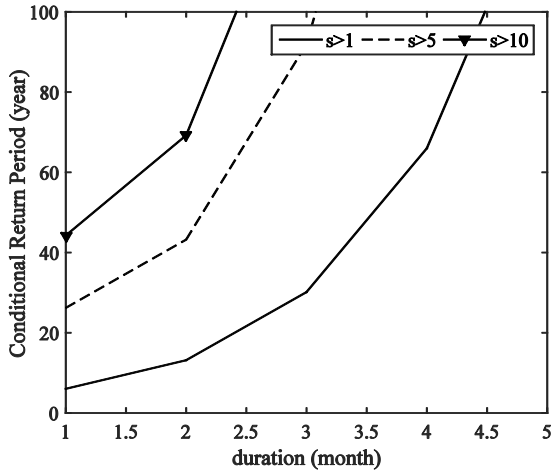
(a)



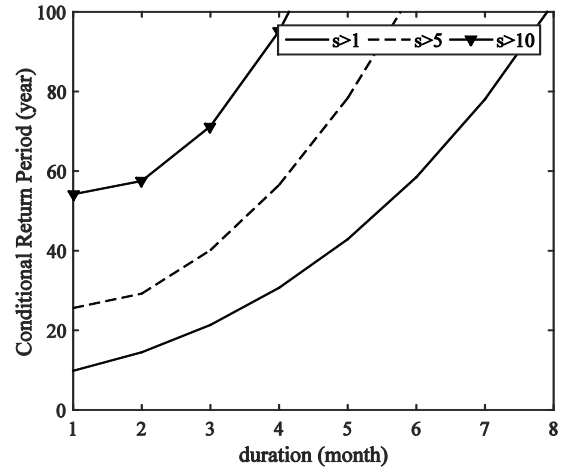
(b)



(c)



(d)



(e)

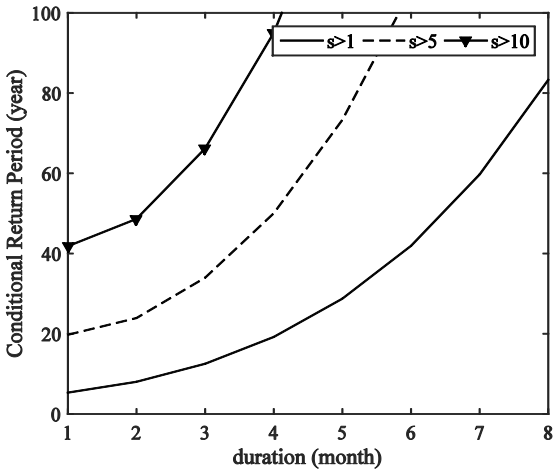
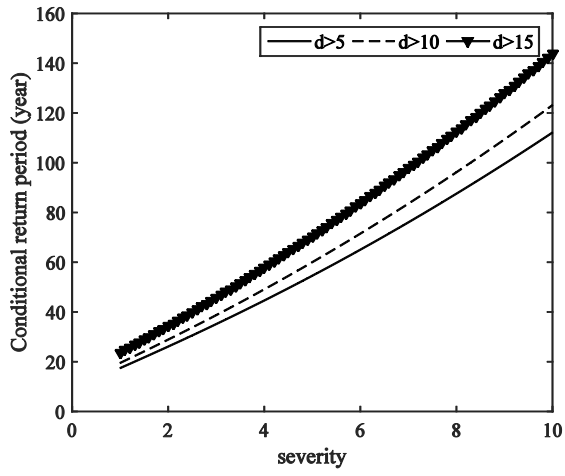
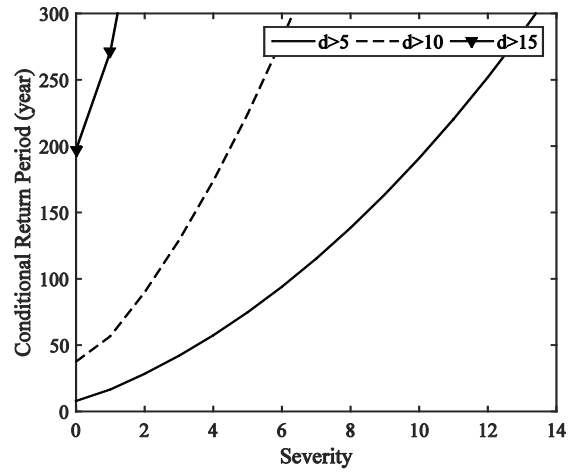


**Fig. 13** Conditional return period of drought duration for a given drought severity,  $s$ , where  $s \geq s'$ ,  $s'=1, 5, 10$ : (a) base period, (b) 2050s under RCP4.5, (c) 2080s under RCP4.5, (d) 2050s under RCP8.5, (e) 2080s under RCP8.5

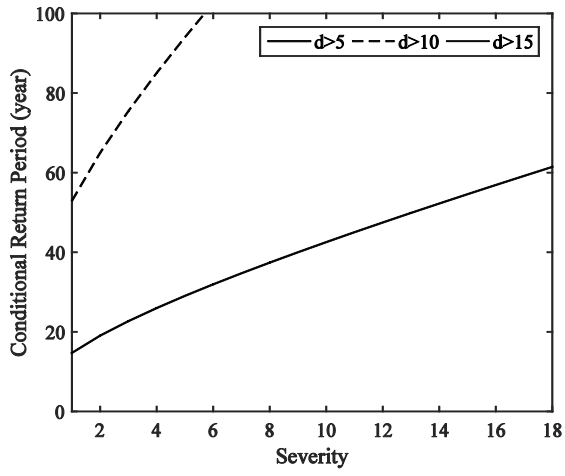
(a)



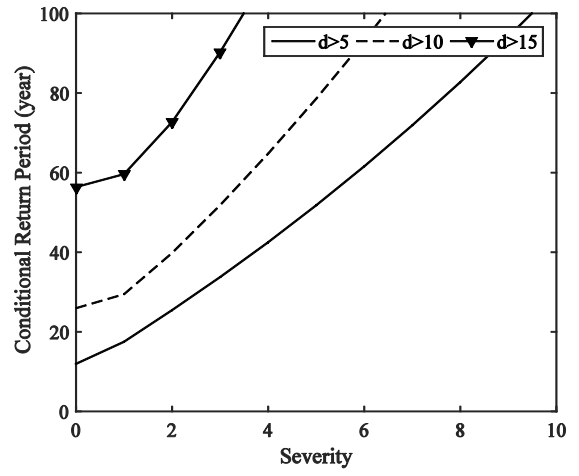
(b)



(c)



(d)



(e)

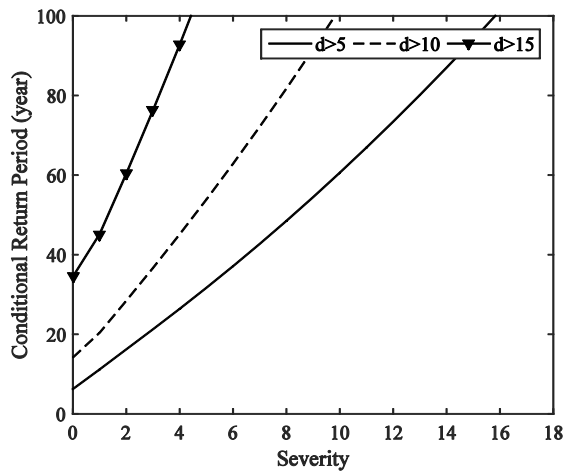


Fig. 14. Conditional return period of drought severity for a given drought duration,  $d$ , where  $d \geq d'$ ,  $d' = 5, 10, 15$ : (a) base period, (b) 2050s under RCP4.5, (c) 2080s under RCP4.5, (d) 2050s under RCP8.5, (e) 2080s under RCP8.5

## 5 Conclusions

Drought analysis was conducted for the Kamal-Saleh basin as a semi-arid area threatened by droughts. The study investigated the impact of climate change on future hydro-meteorological droughts in the study area. Between five GCMs, which were the most widely used in the region, CanESM2 model was chosen as the optimum model to predict the future climate change compared to other GCMs in the region by using the hindcasting approach. This model under RCP's scenarios (RCP4.5 and RCP8.5) was used to analyze drought for two future periods (2050s and 2080s).

For drought assessing and monitoring, the monthly values of SDI and SPI calculated for the studied basin. Subsequently, the historical and future values of the ADI estimated by the PCA method.

After examining and proving the existence of positive correlation between the drought severity and duration, these variables were fitted with their corresponding marginal distributions and the lognormal selected as the best optimal distribution function.

In the next step, in order to analyze the joint probabilities and return period of drought duration and severity, among five common copula functions, the most optimal one in each periods and scenarios was applied to produce the joint and conditional return periods of the in the historical and future periods. In the future scenarios, the probability of occurrence more severe and longer drought was obtained significantly higher than in the baseline periods.

According to ADI, the study area will experience more frequent drought when either duration or severity exceeding certain levels ( $T'_{DS}$ ) for all cases, especially during 2080s under RCP8.5. But return periods estimated by duration and severity exceeding certain levels ( $T_{DS}$ ) will significantly increase for future periods under RCP4.5, while with the same return periods, severe droughts will occur with shorter durations under RCP8.5.

The results of conditional return period of drought characteristics indicate that in future periods, the conditional return periods of a particular duration/severity with a given severity/duration decrease in 2080s compare to 2050s also under RCP8.5 compare to RCP4.5. The conditional return periods of drought severity and duration provided useful information to predict and prevent the destructive effects of drought. Each return period describes different situations; hence, depending on the type of drought danger, the type of return period should be selected.

It can be interpreted from the study that drought is a serious issue in this region and analysis of bivariate joint and conditional return periods of drought will provide valuable information on development and management of water resources. This work shows that the studied basin would be exposed to considerable future droughts as a negative impact of climate change. Therefore, it is essential to make a management plan to reduce its probable negative effects.

## 6 Declarations

**Funding** The authors did not receive support from any organization for the submitted work.

**Conflicts of interest** All Authors declare that they have no conflict of interest.

**Availability of data and material** Available on request.

**Code availability** Not applicable.

**Authors' contributions** This research is conducted as a part of master's degree thesis work of Zahra Fahimirad under the supervision of Nazanin Shahkarami. Both authors have contributed equally to the research.

**Ethics approval** Compliance with Ethical Standards

**Consent to participate** Not applicable.

**Consent for publication** All Authors declare that they agreed with the content and give explicit consent for publication.

## References

1. Azam, M., Seung, M., Jin, M., Hyung, K., and Ardasher, M. 2018. "Copula-Based Stochastic Simulation for Regional Drought Risk Assessment in South Korea." *Water (Basel)*, 10(4), 1-29. <https://doi.org/10.3390/w10040359>.

2. Bazrafshan, J., Hejabi, S., and Rahimi, J. 2014. "Drought monitoring using the multivariate standardized precipitation Index (MSPI)." *Water Resour. Manag.*, 28, 1045-1060. <https://doi.org/10.1007/s11269-014-0533-2>.
3. Beersma, J. J., and T. A. Buishand. 2005. "Joint probability of precipitation and discharge deficits in the Netherlands." *Water Resour.*, 40(12). <https://doi.org/10.1029/2004WR003265>.
4. Chen L, Guo S (2019) Copulas and its application in hydrology and water resources. Springer, Singapore
5. Farjad, B., Gupta, A., Sartipizadeh, H., and Cannon, A. J. 2019. "A novel approach for selecting extreme climate change scenarios for climate change impact studies." *Sci. Total Environ.*, 678, 476-485. <https://doi.org/10.1016/j.scitotenv.2019.04.218>.
6. Ghabaei Sough, M., and Mosaedi M. 2013. "Wheat drought monitoring by using generalized Scalogram model at Mashhad and shiraz synoptic stations." *Iranian Journal of Irrigation and Drainage.*, 7(1).23–35.
7. Ghabaei Sough, M., Zare Abyaneh, H., and Mosaedi, A. 2018. "Assessing a Multivariate Approach Based on Scalogram Analysis for Agricultural Drought Monitoring." *Water Resour. Manag.*, 32, 3423–3440. <https://doi.org/10.1007/s11269-018-1999-0>.
8. Genest, C; and Favre, A.C. 2007. "Everything you always wanted to know about copula modeling but were afraid to ask." *J Hydrol Eng.*, 12(4). 347-368. [https://doi.org/10.1061/\(ASCE\)1084-0699\(2007\)12:4\(347\)](https://doi.org/10.1061/(ASCE)1084-0699(2007)12:4(347))
9. Hao, Z., and AghaKouchak, A. 2013. "Multivariate standardized drought index: a parametric multi-index model." *Adv Water Resour.*, 57. 12-18. <https://doi.org/10.1016/j.advwatres.2013.03.009>

10. Hao, Z., and AghaKouchak. A. 2014. "Multivariate multi-index drought monitoring framework" *J. Hydrometeorol.*, 15. 89-101. <https://doi.org/10.1175/JHM-D-12-0160.1>.
11. Hao, Z., A. AghaKouchak., N. Nakhjiri., and A. Farahmand. 2014. "Global integrated drought monitoring and prediction system". *Sci. Data.*, 1, 140001 (2014). <https://doi.org/10.1038/sdata.2014.1>.
12. Hao, Z., and Singh, VP. 2015. "Drought characterization from a multivariate perspective: A review." *J. Hydrol.*, 527. 668–678. <https://doi.org/10.1016/j.jhydrol.2015.05.031>.
13. Hayes, M. J., Svobodo, M. D., Wihite, D. A., and Vanyarkho, O. V. 1998. "Monitoring the 1996 drought using the standardized precipitation index." *Bull. Am. Meteorol. Soc.*, 80. 429-438.
14. IPCC. Climate Change 2014: Synthesis Report. Contribution of Working Groups I, II and III to the Fifth Assessment Report of the Intergovernmental Panel on Climate Change [Core Writing Team, R.K. Pachauri and L.A. Meyer (eds.)]. IPCC, Geneva, Switzerland, 151 pp.
15. Jain, V., Pandey, R., K.Jain, M., and RyongByun, H. 2015. "Comparison of drought indices for appraisal of drought characteristics in the Ken River Basin." *Weather. Clim. Extremes.*, 8. 1-11. <https://doi.org/10.1016/j.wace.2015.05.002>.
16. Joe, H. 1997. "Multivariate Models and Dependence Concepts", *Chapman & Hall.*, London.
17. Keyantash, J., and Dracup. A. 2004. "An aggregate drought index: Assessing drought severity based on fluctuations in the hydrologic cycle and surface water storage." *Water Resour. Res.*, 40. 1-13. <https://doi.org/10.1029/2003WR002610>.

18. Kim, T. W., Valdés, J. B., and Yoo, C. 2003. "Nonparametric approach for estimating return periods of droughts in arid regions." *J Hydrol Eng.*, 8. 237–246. [https://doi.org/10.1061/\(ASCE\)1084-0699\(2003\)8:5\(237\)](https://doi.org/10.1061/(ASCE)1084-0699(2003)8:5(237)).
19. Kundu, A., Patel, N.R., and Denis, D.M. 2020. "An Estimation of Hydrometeorological Drought Stress over the Central Part of India using Geo-information Technology." *J Indian Soc Remote Sens.*, 48, 1–9. <https://doi.org/10.1007/s12524-019-01048-9>.
20. Kwak, J., Kim, S., Singh, V., Soo Kim, H., Kim, D., Hong, S., and Lee, K. 2015. "Impact of Climate Change on Hydrological Droughts in the Upper Namhan River Basin, Korea." *KSCE J. Civ. Eng.*, 19, 376-384. <https://doi.org/10.1007/s12205-015-0446-5>.
21. Kwon, M., Kwon, H., and Han, D. 2019. "Spatio-temporal drought patterns of multiple drought indices based on precipitation and soil moisture: A case study in South Korea" *Int J Climatol.*, 39, 4669-4687. <https://doi.org/10.1007/s12524-019-01048-9>.
22. Laio, F. 2004. "Cramer-von Mises and AndersonDarling goodness of fit tests for extreme value distributions with unknown parameters." *Water Resour. Res.*, 40, 1-10. <https://doi.org/10.1029/2004WR003204>.
23. Li, Q., P. Li, H., and M. Yu. 2015. "Drought assessment using a multivariate drought index in the Luanhe River basin of Northern China." *Stoch Environ Res Risk Assess.*, 29, 1509–1520. <https://doi.org/10.1007/s00477-014-0982-4>.
24. Loukas, A., and Vasiliades, L. 2005. "Identification of the relationship between meteorological and hydrological drought." April 24 - April 29, Vienna, Austria. *Geography Research Abstract.*, 7. 1-10.
25. McKee, T. B., Doesken, N. J., and Kliest, J. "The relationship of drought frequency and duration to time scales." *8<sup>th</sup> conference on Applied climatology*, Boston, MA, 1993.

26. Meyer, S. J., Hubbard, K. G., and Wilhite, D. A. 1991. "The relationship of climatic indices and variables to corn (maize) yields: a principal components analysis." *Agr. Forest Meteorol.*, 55(1–2). 59-84.
27. Nazemi, A., and Elshorbagy, A. 2012. "Application of copula modelling to the performance assessment of reconstructed watersheds." *Environ Res Risk Assess.*, 26, 189–205. <https://doi.org/10.1007/s00477-011-0467-7>.
28. Nelsen, R. B. 2006. "An introduction to Copulas." *Springer*, New York, 269 pp.
29. Rajsekhar, D., Singh, V.p., and A. K. Mishra. 2014. "Multivariate drought index: An information theory based approach for integrated drought assessment." *J. Hydrol.* 3(1). 64-88. <https://doi.org/10.1016/j.jhydrol.2014.11.031>.
30. Rezaeianzadeh, M., Stein, A., and Cox, J.P. 2016. "Drought Forecasting using Markov Chain Model and Artificial Neural Networks." *Water Resour Manage.*, 30, 2245–2259. <https://doi.org/10.1007/s11269-016-1283-0>.
31. Salvadori, G., and Michele, C.D. 2007. "On the use of copulas in hydrology: theory and practice" *J Hydrol Eng*, 12(4). [https://doi.org/10.1061/\(ASCE\)1084-0699\(2007\)12:4\(369\)](https://doi.org/10.1061/(ASCE)1084-0699(2007)12:4(369)).
32. Shiau, J. T. 2006. "Fitting drought duration and severity with two-dimensional copulas." *Water Resour Manage.*, 20, 795-815. <https://doi.org/10.1007/s11269-005-9008-9>.
33. Sklar, M. 1959. "Fonctions de repartition an dimensions et leurs marges." *Publ. Inst. Statist. Univ. Paris.*, 8, 229–231.
34. Svoboda, M., LeCompte, D., Hayes, M., and Heim, R. 2002. "The drought monitor." *Bull. Am. Meteorol. Soc.*, 83, 1181. <https://doi.org/10.1175/1520-0477-83.8.1181>
35. Wilks, D. S. 2011. "Statistical Methods in the Atmospheric Sciences." *Academic Press*. California. 100. 3<sup>rd</sup> Edition.

36. Xia, Y., M. B. Ek., Peters-Lidard, C. D., Mocko, D., Svoboda, M., Sheffield, J., and Wood, E.F. 2014. "Uncertainties, Correlations, and Optimal Blends of Drought Indices from the 934 NLDAS Multiple Land Surface Model Ensemble" *J. Hydrometeorol.* 15. 1636–1650. <https://doi.org/10.1175/JHM-D-13-058.1>.
37. Yevjevich, V and Ingenieur, J. 1967. "An Objective Approach to Definitions and Investigations of Continental Hydrologic Droughts" Colorado State University, Fort Collins, Colo, USA.
38. Yu, M., Li, Q., Lu, G., Wang, H., and Li, P. 2015. "Development and application of a short-/long-term composited drought index in the upper Huaihe river basin, China." *the International Association of Hydrological Sciences.*, 369.103–108. <https://doi.org/10.5194/piahs-369-103-2015>.
39. Yusof, F., Hui-Mean, F., Suhaila, J., and Yusof, Z. 2013. "Characterisation of Drought Properties with Bivariate Copula Analysis." *Water Resour. Manag.*, 27, 4183–4207. <https://doi.org/10.1007/s11269-013-0402-4>.

# Figures

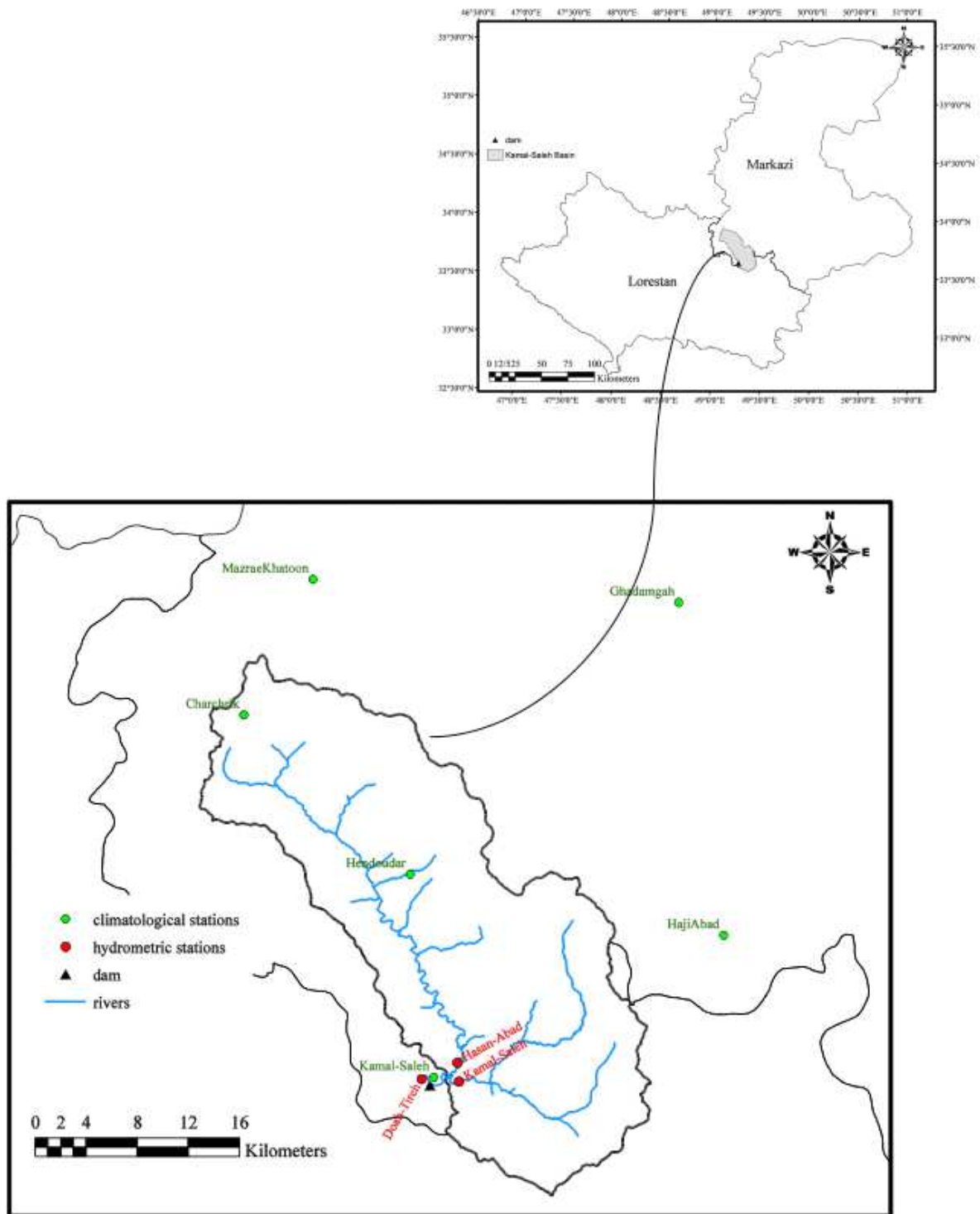
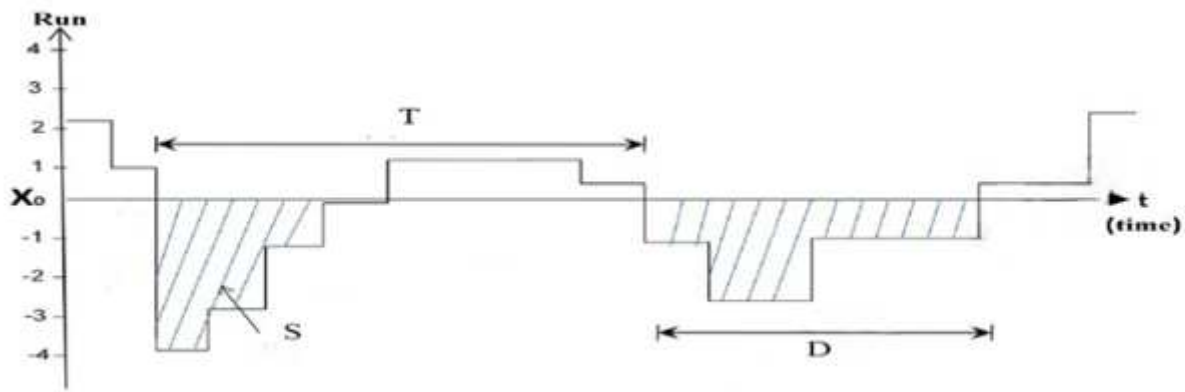


Figure 1

The study basin and stations. Note: The designations employed and the presentation of the material on this map do not imply the expression of any opinion whatsoever on the part of Research Square

concerning the legal status of any country, territory, city or area or of its authorities, or concerning the delimitation of its frontiers or boundaries. This map has been provided by the authors.



**Figure 2**

Definition sketch of drought characteristics showing two drought events (Yevjevich and Ingenieur, 1967)

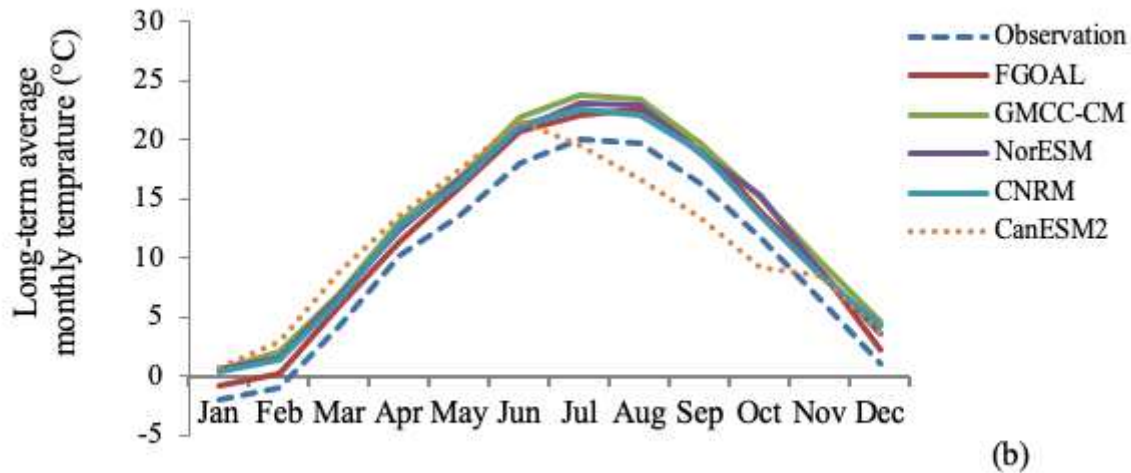
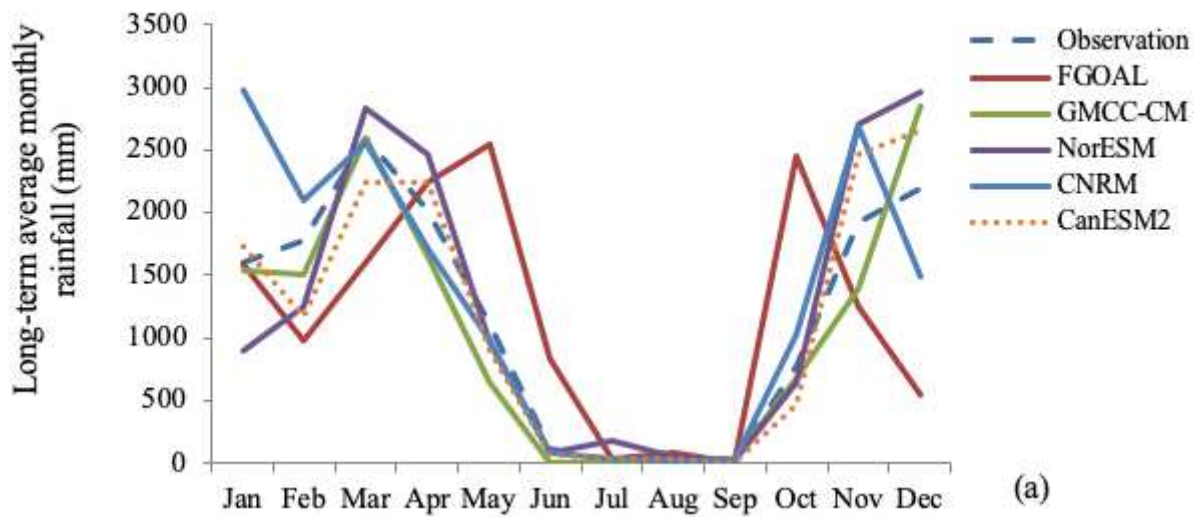


**Figure 3**

Comparison of long-term average of monthly rainfall and temperature values in the base period: (a) rainfall (b) temperature

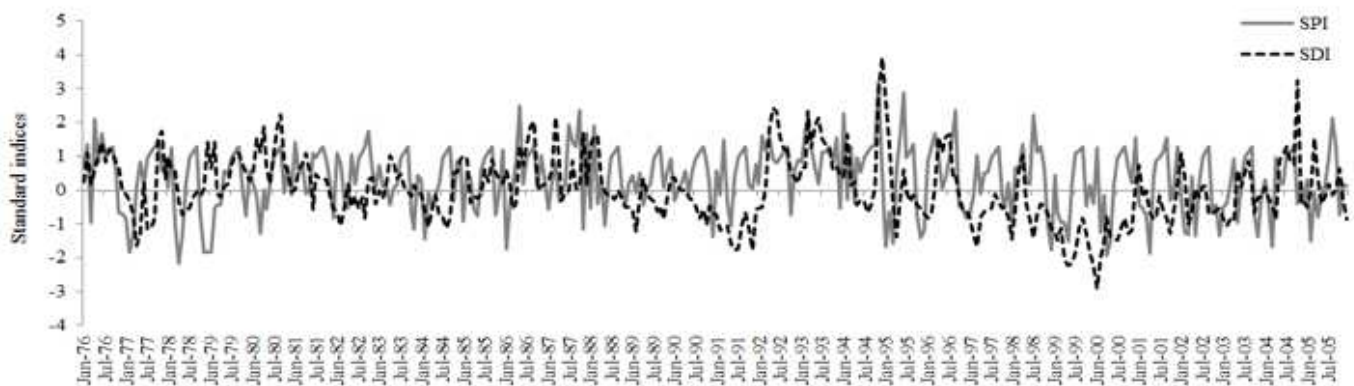


**Figure 4**

The monthly SPI and SDI (base period) for region studied

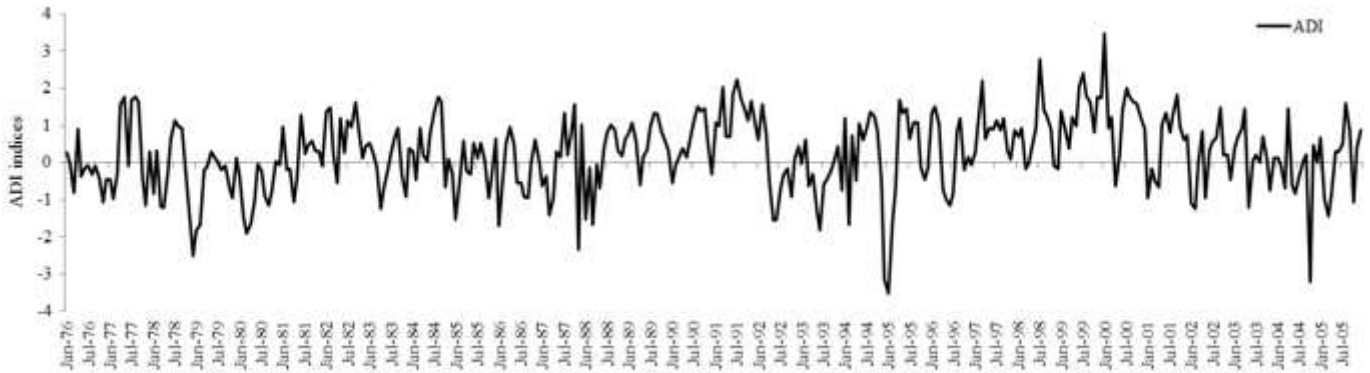


**Figure 5**

The monthly ADI (base period)

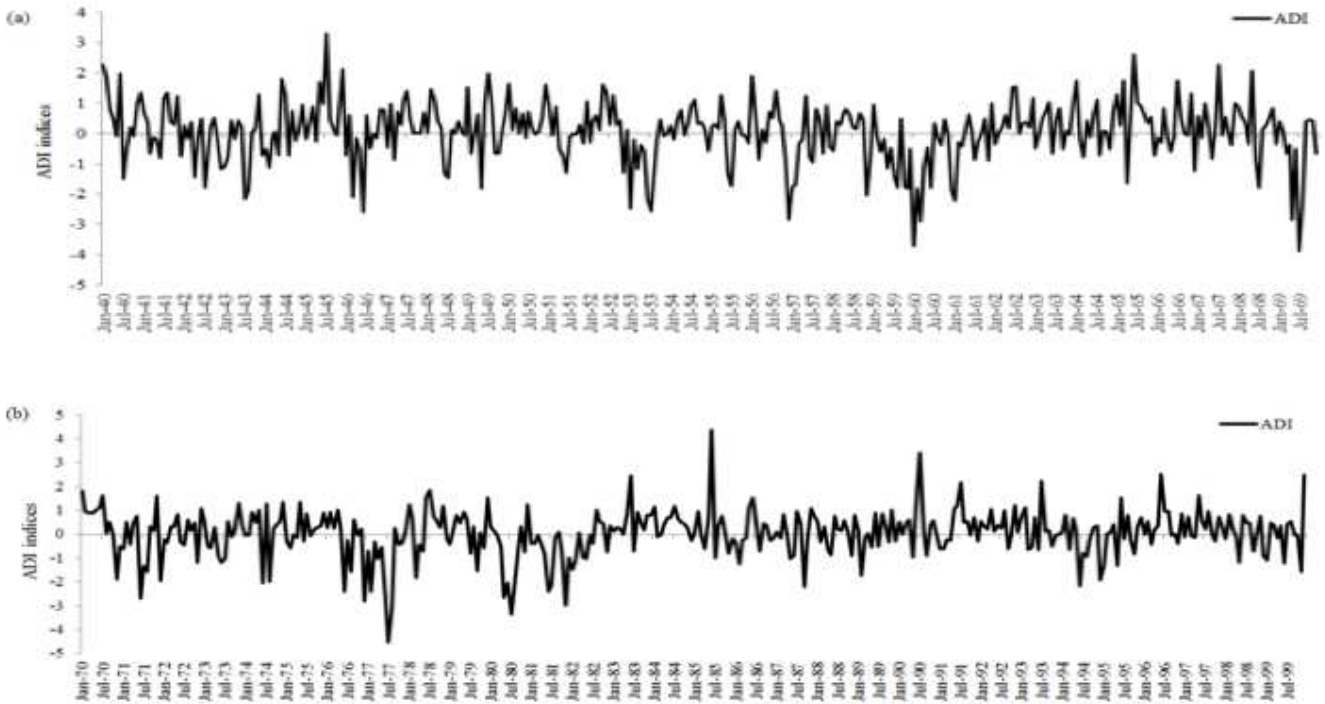


**Figure 6**

Comparison of ADI for two future periods under RCP4.5 (a) 2050s (b) 2080s

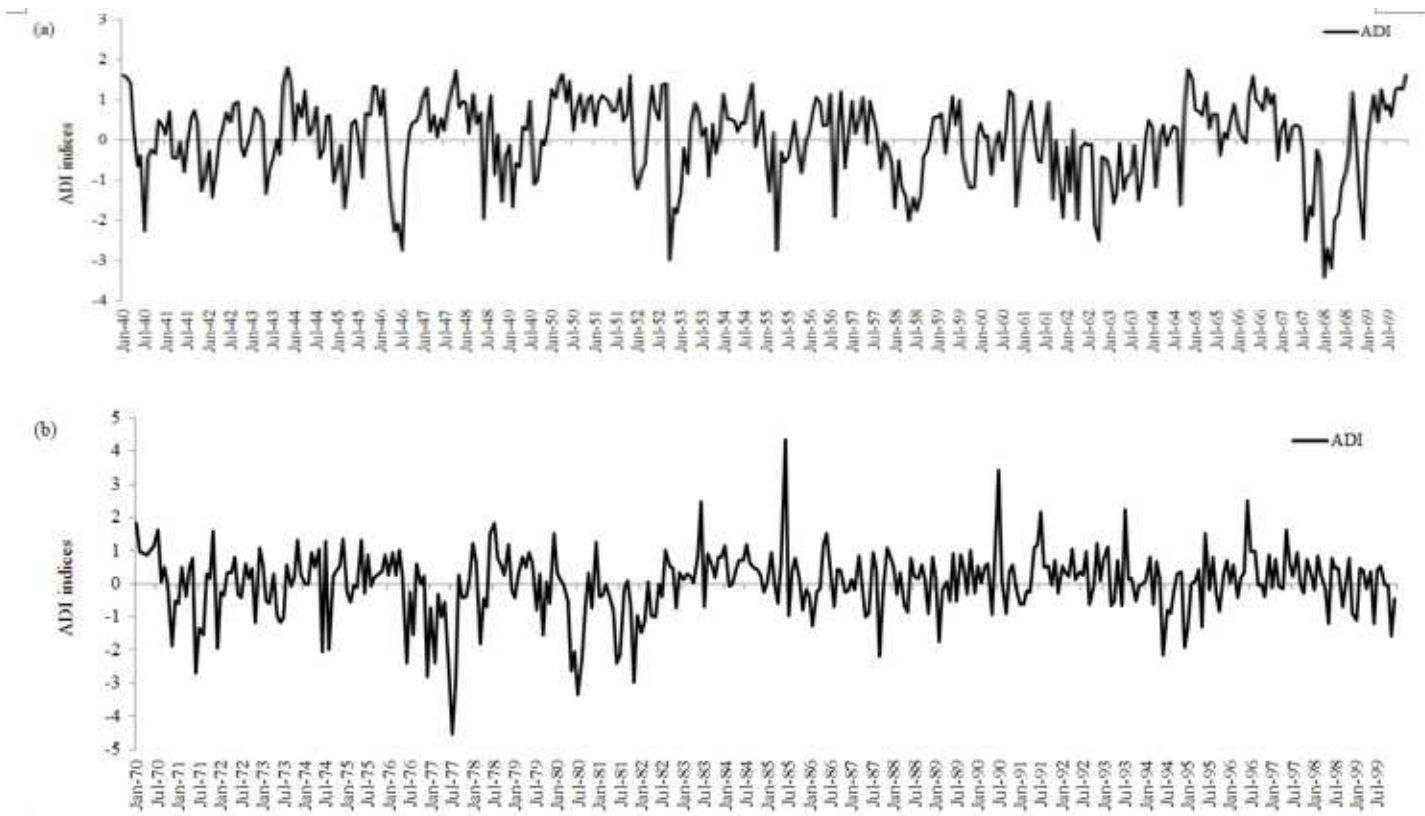


**Figure 7**

Comparison of ADI for two future period under RCP8.5 (a) 2050s (b) 2080s

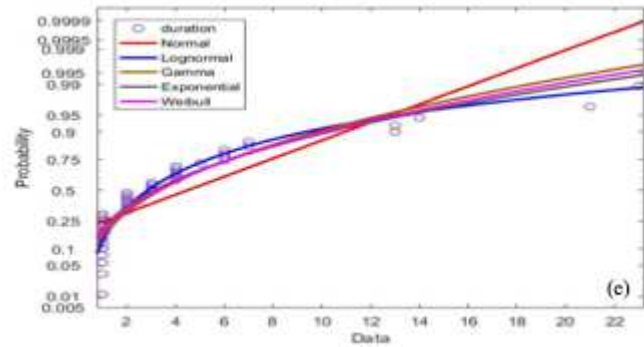
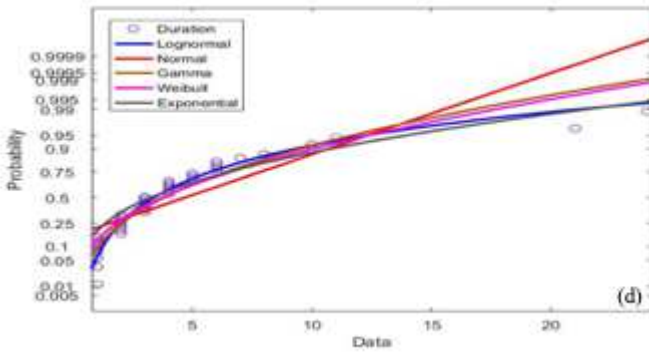
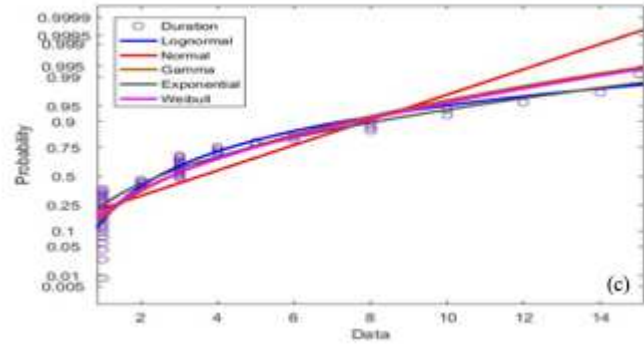
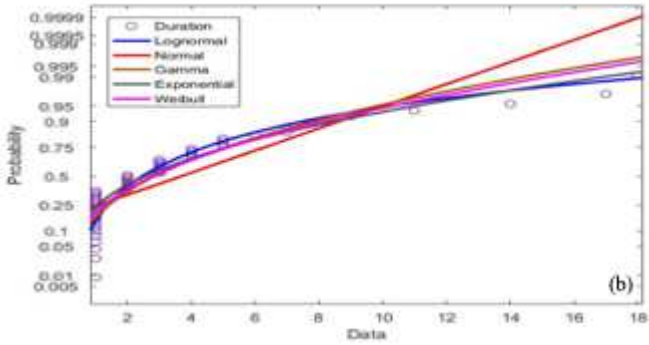
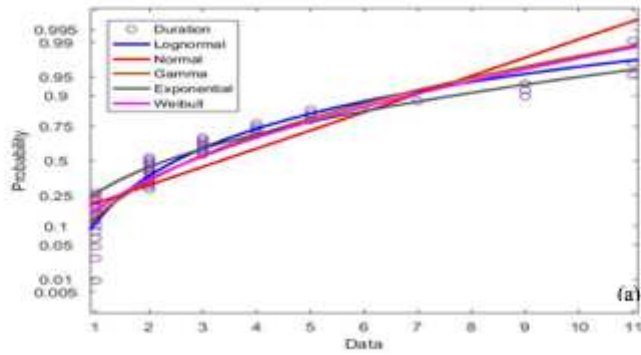


**Figure 8**

Comparison between the best-fitted marginal distributions for drought duration (a) base period, (b) 2050s under RCP4.5, (c) 2080s under RCP4.5, (d) 2050s under RCP8.5, (e) 2080s under RCP8.5

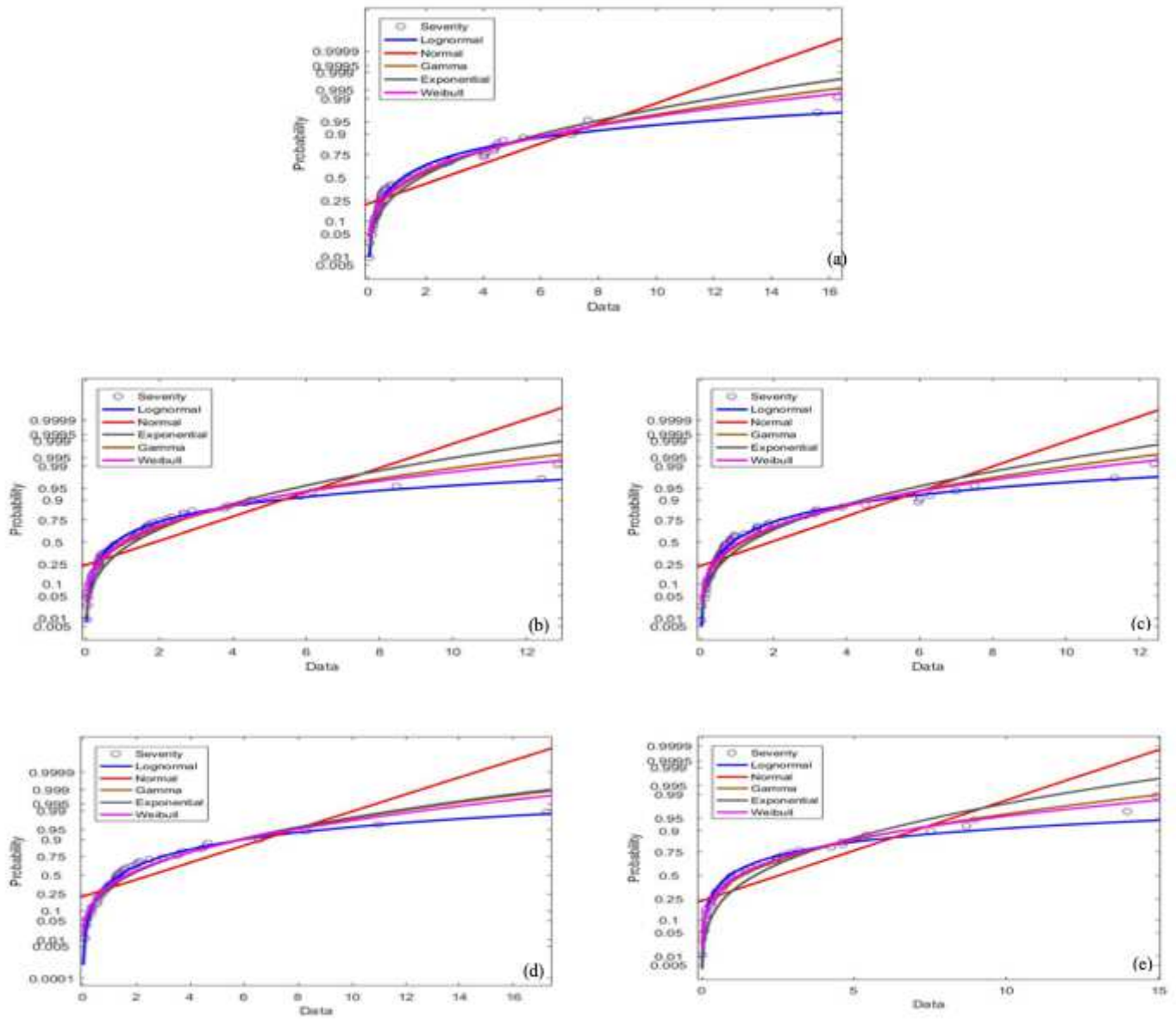


**Figure 9**

Comparison between the best-fitted marginal distributions for drought severity (a) base period, (b) 2050s under RCP4.5, (c) 2080s under RCP4.5, (d) 2050s under RCP8.5, (e) 2080s under RCP8.5

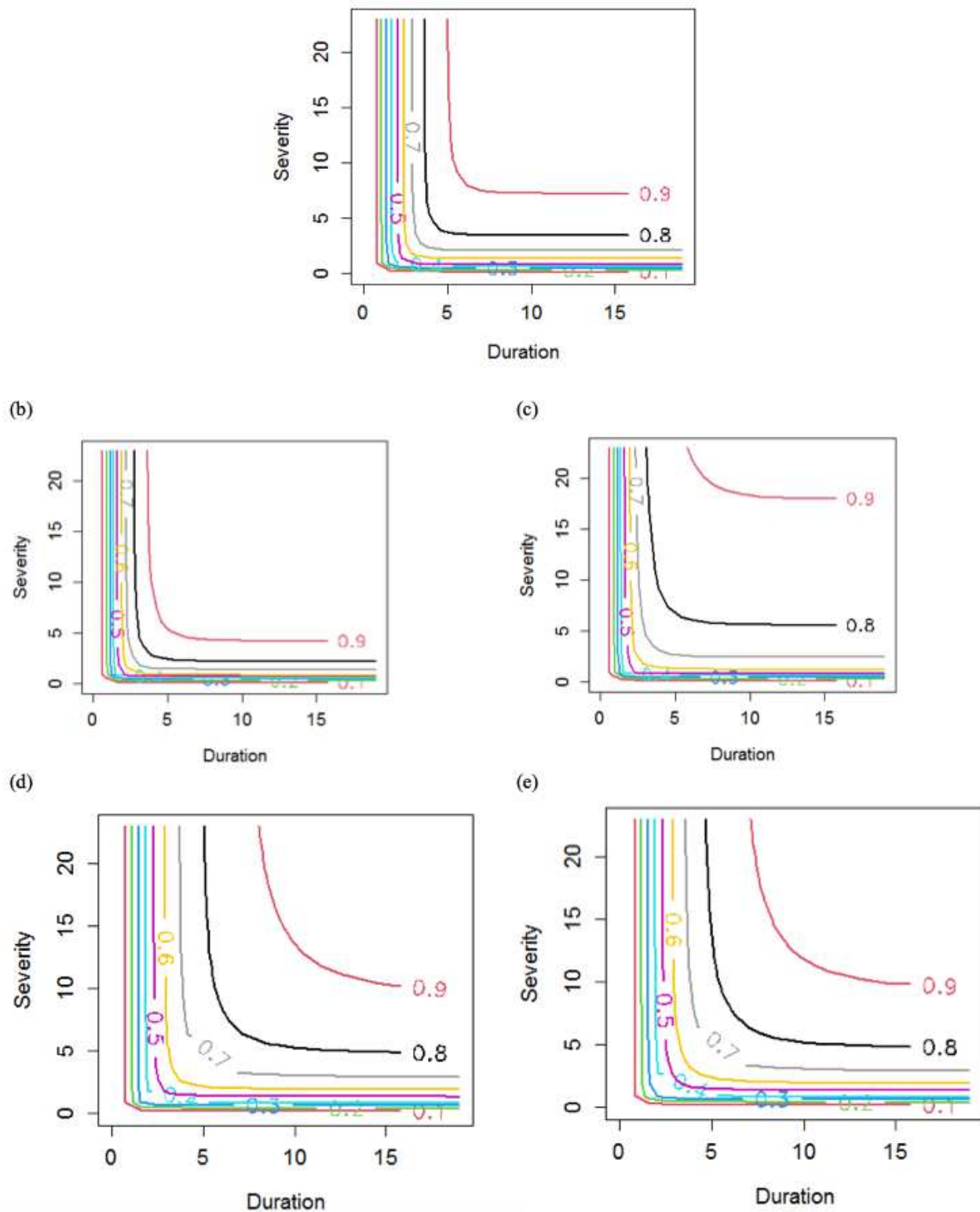
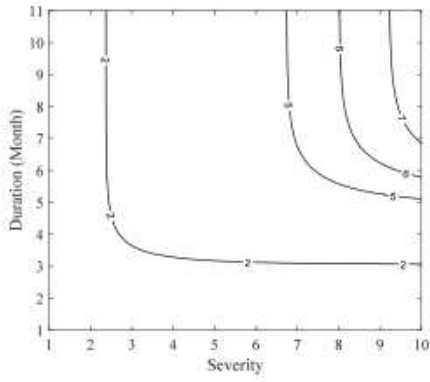


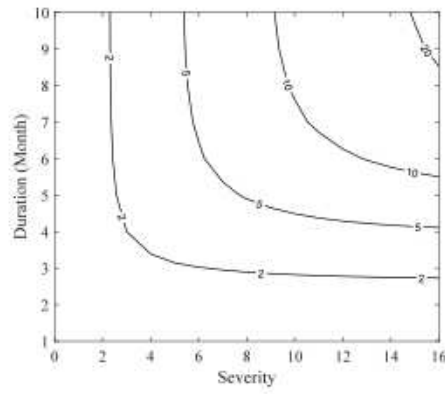
**Figure 10**

Contours of joint probabilities of drought severity and duration for (a) base period, (b) 2050s under RCP4.5, (c) 2080s under RCP4.5, (d) 2050s under RCP8.5, (e) 2080s under RCP8.5

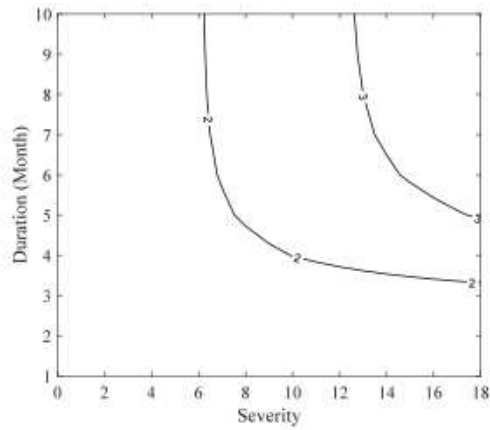
(a)



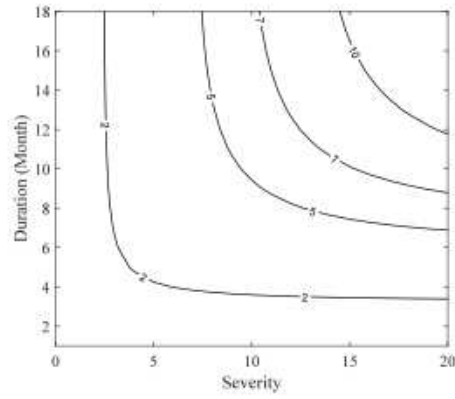
(b)



(c)



(d)



(e)

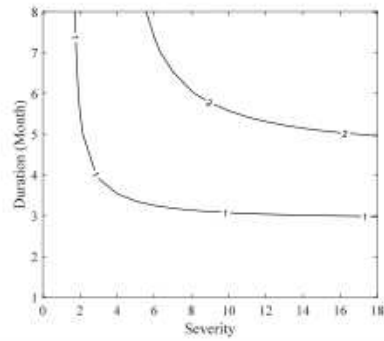
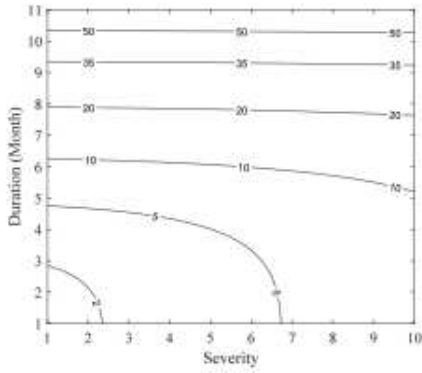


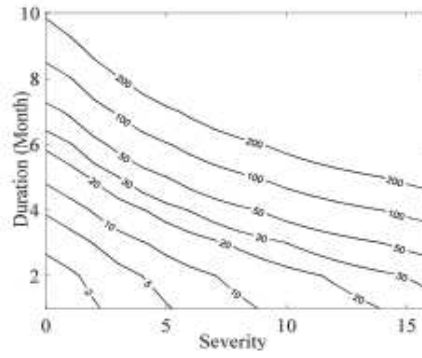
**Figure 11**

Joint return period of drought duration or severity exceeding certain levels  $\bar{\lambda}(T_{DS}^*)$  for (a) base period, (b) 2050s in RCP4.5, (c) 2080s in RCP4.5, (d) 2050s in RCP8.5, (e) 2080s in RCP8.5

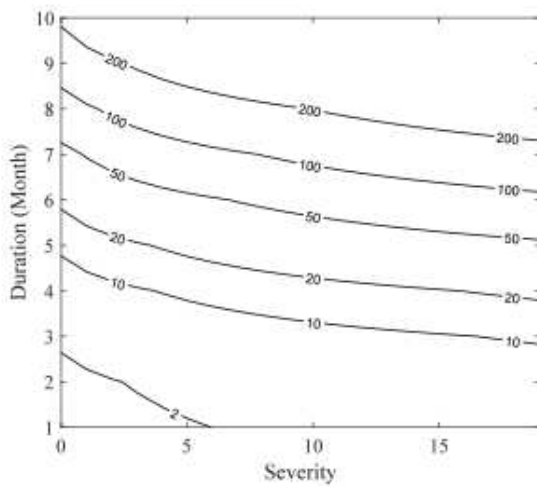
(a)



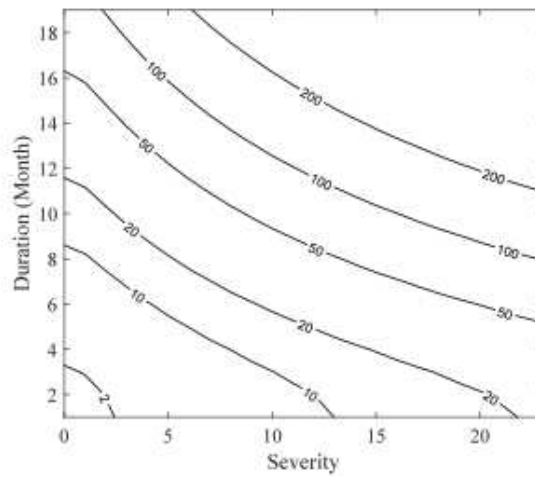
(b)



(c)



(d)



(e)

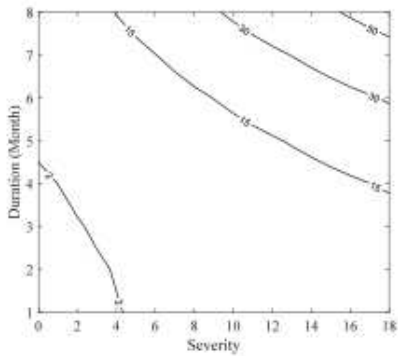
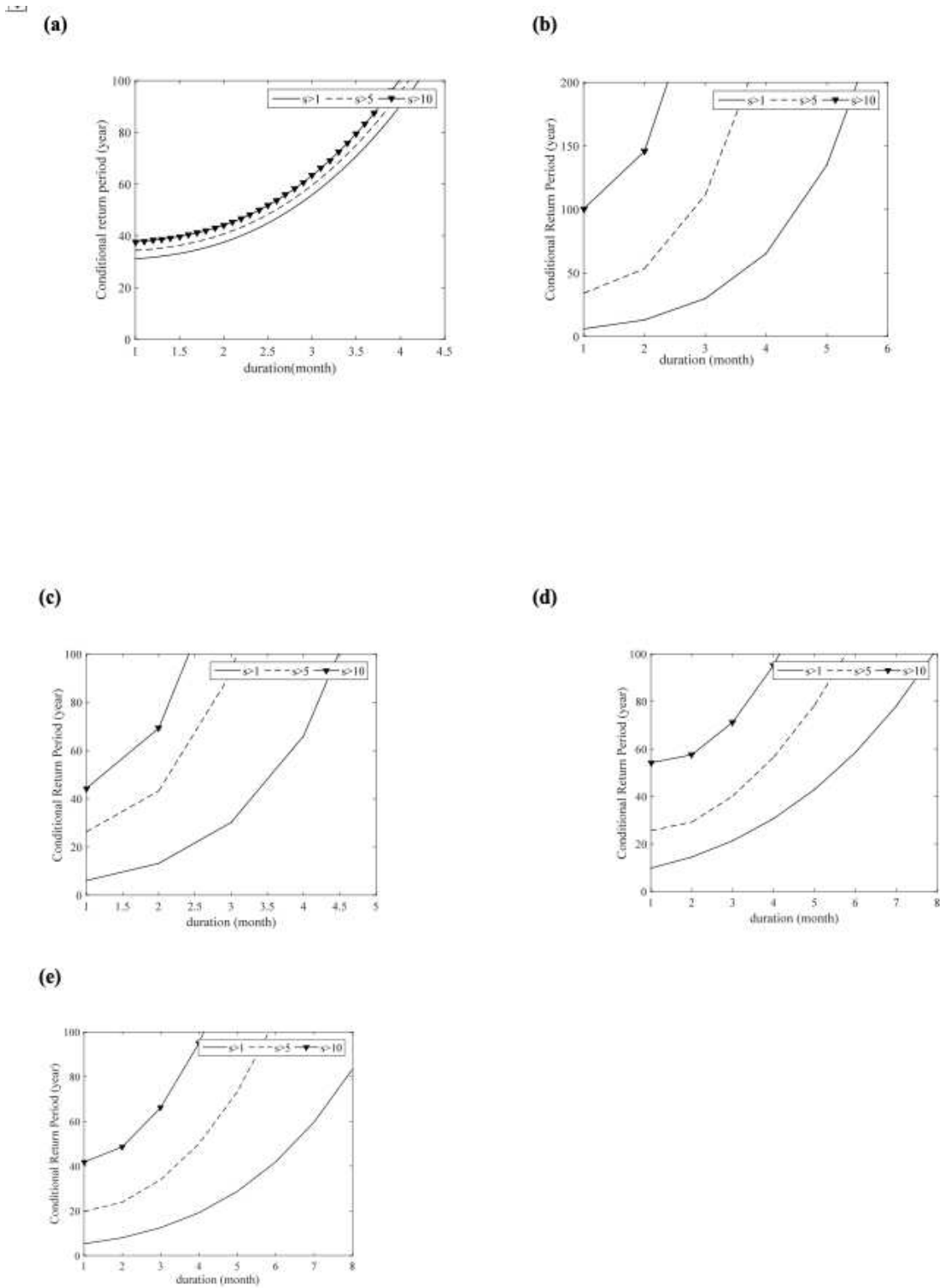


Figure 12

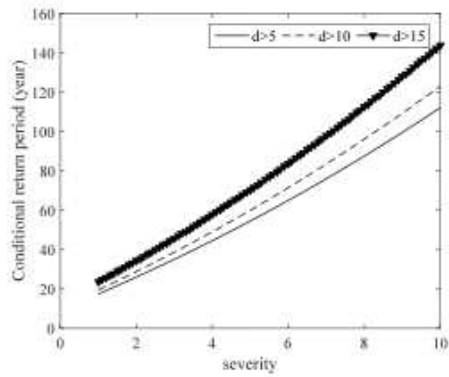
Joint return period of drought duration and severity both exceeding certain levels  $\lambda(T_{\lambda}DS)$  for (a) base period, (b) 2050s under RCP4.5, (c) 2080s under RCP4.5, (d) 2050s under RCP8.5, (e) 2080s under RCP8.5



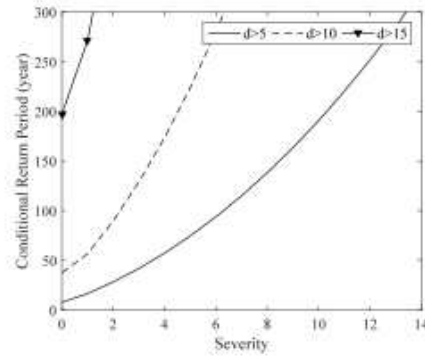
**Figure 13**

Conditional return period of drought duration for a given drought severity,  $s$ , where  $s \geq s_{\text{crit}}$ ,  $s_{\text{crit}}=1, 5, 10$ : (a) base period, (b) 2050s under RCP4.5, (c) 2080s under RCP4.5, (d) 2050s under RCP8.5, (e) 2080s under RCP8.5

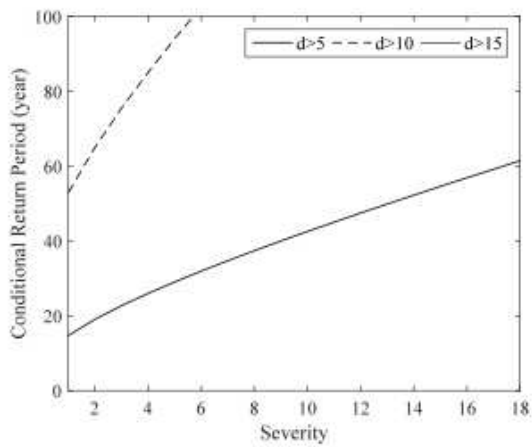
(a)



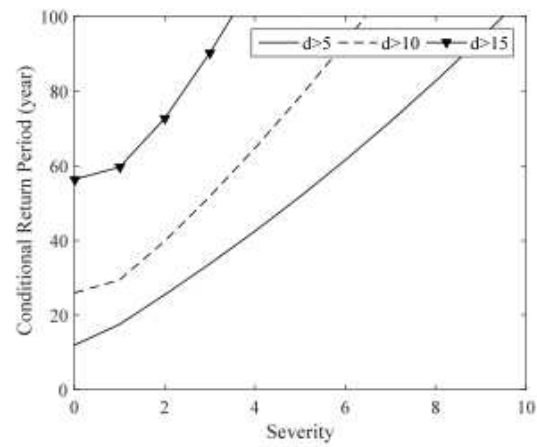
(b)



(c)



(d)



(e)

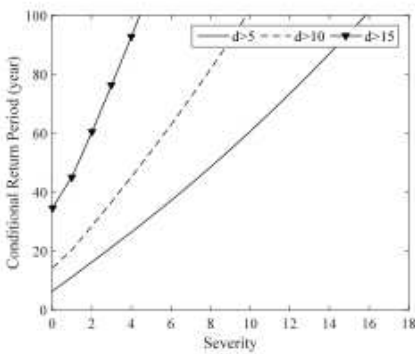


**Figure 14**

Conditional return period of drought severity for a given drought duration,  $d$ , where  $d \geq d_0$ ,  $d_0 = 5, 10, 15$ : (a) base period, (b) 2050s under RCP4.5, (c) 2080s under RCP4.5, (d) 2050s under RCP8.5, (e) 2080s under RCP8.5